NASA/TM—97-206307

The Implicit and Explicit a–μ Schemes

Sin-Chung Chang
Lewis Research Center, Cleveland, Ohio

Ananda Himansu
Cleveland Telecommunications Corporation, Solon, Ohio

National Aeronautics and
Space Administration

Lewis Research Center

November 1997

Available from

NASA Center for Aerospace Information
800 Elkridge Landing Road
Linthicum Heights, MD 21090-2934
Price Code: A04

National Technical Information Service
5287 Port Royal Road
Springfield, VA 22100
Price Code: A04

The Implicit and Explicit a-μ Schemes

S.C. Chang[1] and A. Himansu[2]
[1] NASA Lewis Research Center, Cleveland, Ohio 44135, USA
[2] Cleveland Telecommunications Corporation, Solon, Ohio 44139, USA

Abstract

Artificial numerical dissipation is an important issue in large Reynolds number computations. In such computations, the artificial dissipation inherent in traditional numerical schemes can overwhelm the physical dissipation and yield inaccurate results on meshes of practical size. In the present work, the space-time conservation element and solution element method is used to construct new and accurate numerical schemes such that artificial numerical dissipation will not overwhelm physical dissipation. Specifically, these schemes have the property that numerical dissipation vanishes when the physical viscosity goes to zero. These new schemes therefore accurately model the physical dissipation even when it is extremely small. The method of space-time conservation element and solution element, currently under development, is a nontraditional numerical method for solving conservation laws. The method is developed on the basis of local and global flux conservation in a space-time domain, in which space and time are treated in a unified manner. Explicit solvers for model and fluid dynamic conservation laws have previously been investigated. In this paper, we introduce a new concept in the design of implicit schemes, and use it to construct two highly accurate solvers for a convection-diffusion equation. The two schemes become identical in the pure convection case, and in the pure diffusion case. The implicit schemes are applicable over the whole Reynolds number range, from purely diffusive equations to purely inviscid (convective) equations. The stability and consistency of the schemes are analysed, and some numerical results are presented. *It is shown that, in the inviscid case, the new schemes become explicit and their amplification factors are identical to those of the Leapfrog scheme. On the other hand, in the pure diffusion case, their principal amplification factor becomes the amplification factor of the Crank-Nicolson scheme.* We also construct an explicit solver with the treatment of diffusion being based on that in the implicit solvers. The explicit solver has only a CFL stability limitation on the Courant number, yet it retains the second-order spatial accuracy of the implicit schemes.

1 Introduction

The method of space-time conservation element and solution element (the CE/SE method, for short) is a new numerical discretization method for solving conservation laws ([1]-[27]). The distinguishing features of the method are (i) an emphasis on solving a general space-time integral form of the conservation laws, (ii) the requirement of local and global conservation of space-time fluxes as a basis for the method, (iii) the construction of numerical schemes so as to reflect the initial-value/boundary-value nature and invariance properties of the governing equations, (iv) use of only the simplest discretization stencils, (v) the absence of upwind-biasing of fluxes and approximate Riemann solvers with their attendant complexities, (vi) the absence of directional splitting techniques and the difficulties associated with them, for flow computations in multiple spatial dimensions, and (vi) the treatment of flow property gradients as additional unknowns, thus eliminating the need for gradient reconstruction using ad hoc polynomial fitting and flux limiters. Reference [11] is a review of the CE/SE method that details the differences between the CE/SE method and the traditional numerical methods for conservation laws.

Based upon the physics of a scalar convection equation, [6] contains a discussion of the requirements for a numerical scheme to be an ideal solver for such a conservation law. The desirability of the distinguishing features mentioned in the previous paragraph follows from the requirements listed in [6], and from an emphasis in the CE/SE method on simplicity, generality and accuracy. With these requirements and this emphasis as guiding principles, several two-level explicit schemes were constructed in [6, 4] to solve (i) the pure convection equation

$$\frac{\partial u}{\partial t} + a\frac{\partial u}{\partial x} = 0 \tag{1.1}$$

with given initial values, and (ii) the convection-diffusion equation

$$\frac{\partial u}{\partial t} + a\frac{\partial u}{\partial x} - \mu\frac{\partial^2 u}{\partial x^2} = 0 \tag{1.2}$$

with given initial and boundary values. In the foregoing equations, the convection velocity a, and the viscosity coefficient μ (> 0) are constants. These schemes were then extended to solve the 1-D time-dependent Euler and Navier-Stokes equations of a perfect gas [6, 4]. Moreover, except for the Navier-Stokes solver, the above 1-D schemes have been generalized to their 2-D counterparts [7, 5]. Because of the inherent simplicity and generality of the current method, the above multidimensional generalization is a straightforward matter. Also, as a result of the similarity in their designs, each of the above 2-D schemes shares with its 1-D version virtually the same fundamental characteristics.

We now discuss the appropriateness of using an implicit, rather than explicit, solver for initial-value/boundary-value problems such as that represented by Eq. (1.2). For a two-level explicit scheme, the value of a solution at any mesh point has a finite domain of dependence

at the previous time level. As an example, consider a finite-difference solver for Eq. (1.1). Let u_j^n, the mesh value of u at any mesh point (j,n) (point P in Fig. 1(a)) be determined by u_{j-1}^{n-1}, u_j^{n-1}, and u_{j+1}^{n-1}. Then the numerical domain of dependence of u_j^n at the $(n-1)$th time level contains three mesh points. Also, one can see that u_j^n is dependent only on the initial data given on the line segment AB.

For an initial-value problem, such as a time-dependent Euler problem or a problem involving Eq. (1.1), the exact solution at any point in space-time also has a finite domain of dependence on the initial plane. As a result, explicit schemes could be ideal solvers for such a problem if they satisfy the requirement that the physical domain of dependence be a subset of the numerical domain of dependence. The latter requirement manifests itself as a CFL stability limit on the Courant number.

On the other hand, the solution of an initial-value/boundary-value problem at any point in space-time is dependent on the initial data and the boundary data up to the time of the point under consideration. As an example, consider a problem involving Eq. (1.2). As shown in Fig. 1(b), the exact solution at point P is dependent on the initial/boundary data given on EC, CD, and DF, where E, P, and F are at the same time level. Let this problem be solved using the explicit scheme that was explained with reference to Fig. 1(a). Let P also be a mesh point (j,n). Then the numerical solution value u_j^n is dependent only on the initial/boundary data given on AC, CD and DB. *It is completely independent of those data given on AE and BF.* Contrarily, if the same problem is solved using an implicit scheme, then u_j^n is dependent on the initial/boundary data given on EC, CD, and DF. In other words, the numerical domain of dependence of the implicit scheme is consistent with the physical domain of dependence of the problem under consideration, while that of the explicit scheme is not.

Two observations can be made as a result of the above discussions.

(a) Generally speaking, an explicit scheme is not an ideal solver for an initial-value/boundary-value problem. Because a time-dependent Navier-Stokes problem is such a problem, the above argument implies that an explicit scheme cannot be used to solve a time-dependent Navier-Stokes problem except for the special circumstance in which errors caused by neglecting certain initial/boundary data (such as those given on AE and BF in Fig. 1(a)) are relatively small. The factors that help achieve the above special circumstance include: (i) a small time-step size to spatial-mesh interval ratio, (ii) a small time rate of change of boundary data, and (iii) a small contribution of the viscous terms in the Navier-Stokes equations relative to that of the inertial terms. Note that condition (iii) may be met by a high-Reynolds-number flow. Under the special circumstance when an explicit solver may be used, such a solver may have the advantage of being computationally less expensive than an implicit solver for the same problem.

(b) Generally, an implicit scheme is not an ideal solver for an initial-value problem. This is because the domain of dependence in the former is far greater than in the latter. As a result, although an implicit solver meets stability criteria, the resulting solution tends to be

contaminated by extraneous information.

With these considerations in mind, in this paper we will construct and analyse two implicit solvers for Eq. (1.2). For reasons (including remark (b) above) that will be explained in Section 3, the implicit solvers will be constructed in such a way that when the viscosity coefficient μ vanishes, the schemes will become an explicit scheme for Eq. (1.1), termed the a scheme, that was described in [6]. A special case of the implicit schemes was described without analysis in [8]. We will also construct and analyse an explicit scheme which also, in the inviscid case, reduces to the a scheme. The explicit scheme is suitable as a solver for Eq. (1.2) either when the time-step to spatial-mesh-interval ratio is small enough, or when the time rate of change of boundary data is zero and only a 'steady-state' limit of the solution is of interest.

The CE/SE explicit solvers referred to earlier, and the implicit and explicit solvers to be described herein, are all built on a foundation of flux conservation in space-time. Although the differential equation representing a conservation law is used in the CE/SE method, emphasis is placed on a space-time integral form of the conservation law. In the following paragraphs, we explain the space-time integral formulation of conservation laws.

Let Eqs. (1.1) and (1.2) be in dimensionless form. Let $x_1 = x$ and $x_2 = t$ be considered as the coordinates of a two-dimensional Euclidean space E_2. Consider the integral conservation law

$$\oint_{S(R)} \vec{h} \cdot d\vec{s} = 0. \tag{1.3}$$

Here (i) $S(R)$ is the boundary of an arbitrary space-time region R in E_2 (see Fig. 2), (ii) $\vec{h}$ is a current density vector in E_2, and (iii) $d\vec{s} = d\sigma\, \vec{n}$ with $d\sigma$ and $\vec{n}$, respectively, being the area and the outward unit normal of a surface element on $S(R)$. Note that (i) $\vec{h} \cdot d\vec{s}$ is the *space-time* flux of $\vec{h}$ leaving the region R through the surface element $d\vec{s}$, and (ii) all mathematical operations can be carried out as though E_2 were an ordinary two-dimensional Euclidean space.

If we set

$$\vec{h} = (au, u) \tag{1.4}$$

in Eq. (1.3), then it can be shown that Eq. (1.1) is the differential form of Eq. (1.3), under suitable smoothness assumptions on u. This can be done by using Gauss' divergence theorem in the space-time E_2. If, instead, we set

$$\vec{h} = (au - \mu \frac{\partial u}{\partial x}, u) \tag{1.5}$$

in Eq. (1.3), then it can similarly be shown that Eq. (1.2) is the differential form of Eq. (1.3), again under suitable smoothness assumptions on u. In both cases, Eq. (1.3) is the more fundamental and more general expression of the physical conservation law.

At this juncture, note that the conservation law Eq. (1.3) appears in a form in which space and time are unified and treated on the same footing. *This unity of space and time is a key characteristic that distinguishes the current method from most of the traditional*

methods. It provides flexibility in the shape of the discrete elements over which conservation is enforced. Also, it is the conservation of *space-time flux* that is enforced, rather than the traditional conservation of spatial flux with time evolution possibly being outside the conservation framework.

As mentioned above, the implicit and explicit solvers developed in this paper contain the explicit a scheme for the pure convection equation as a special case. An understanding of the latter scheme is the best route to understanding the properties of the new implicit and explicit solvers. Hence, we review the a scheme in the next section. In Section 3, we develop the discrete conservation equations for the implicit solvers. The solution procedure for each implicit solver is presented in Section 4. The stability of the implicit schemes is discussed in Section 5. The consistency and truncation errors of the implicit schemes are investigated in Section 6. A modification of the initial conditions to improve solution accuracy is described in Section 7. We develop and analyse the new explicit scheme in Section 8. Some numerical examples demonstrating the properties of the new schemes are displayed in Section 9, and we end with a summary of the paper.

2 Review of an Explicit Scheme

In this section, we review the a scheme, which is the inviscid version of the explicit a-μ scheme [6, 4]. The a scheme is a nondissipative solver for the pure convection equation, Eq. (1.1). To achieve consistency of the notations used in this section and the sections that follow, the notations used here will be slightly different from those used in [6, 4].

Let Ω_1 denote the set of mesh points (j, n) in E_2 (dots in Fig. 3) where $n = 0, \pm 1, \pm 2, \pm 3, \ldots$, and, for each n, $j = n, n \pm 2, n \pm 4, , \ldots$. Note that only a finite portion of this unbounded space-time mesh is seen in Fig. 3. We select a numerical representation of the solution that is piecewise linear in the (x, t) coordinates. There is a solution element (SE) associated with each $(j, n) \in \Omega_1$. Let the solution element $\mathrm{SE}(j, n)$ be the *space-time* region bounded by the dashed curve depicted in Fig. 4. It includes a horizontal line segment, a vertical line segment, and their immediate neighborhood. The exact size and shape of the neighborhood is immaterial to our purpose.

For any $(x, t) \in \mathrm{SE}(j, n)$, $u(x, t)$, and $\vec{h}(x, t)$, respectively, are approximated by $u^*(x, t\,; j, n)$ and $\vec{h}^*(x, t\,; j, n)$ which we shall define shortly. Let

$$u^*(x, t\,; j, n) \stackrel{\text{def}}{=} u_j^n + (u_x)_j^n (x - x_j) + (u_t)_j^n (t - t^n), \tag{2.1}$$

where (i) u_j^n, $(u_x)_j^n$, and $(u_t)_j^n$ are constants in $\mathrm{SE}(j, n)$, and (ii) (x_j, t^n) are the coordinates of the mesh point (j, n). Note that

$$u^*(x_j, t^n; j, n) = u_j^n; \quad \frac{\partial u^*(x, t\,; j, n)}{\partial x} = (u_x)_j^n; \quad \frac{\partial u^*(x, t\,; j, n)}{\partial t} = (u_t)_j^n. \tag{2.2}$$

Moreover, if we identify u_j^n, $(u_x)_j^n$, and $(u_t)_j^n$, respectively, with the values of u, $\partial u/\partial x$, and $\partial u/\partial t$ at (x_j, t^n), the expression on the right side of Eq. (2.1) becomes the first-order

Taylor's expansion of $u(x,t)$ at (x_j, t^n). Thus, u_j^n, $(u_x)_j^n$, and $(u_t)_j^n$ are respectively the numerical analogues of the values of u, $\partial u/\partial x$, and $\partial u/\partial t$ at (x_j, t^n). We mention here that the choice of basis functions for the linear approximation is both convenient and meaningful, because the conservative variable u and its gradient arise naturally in the statement of the conservation law. Numerical solution of an initial value problem for Eq. (1.1) then reduces to determining the three unknown constants in Eq. (2.1) associated with each mesh point (j,n). This will be done by specifying that the numerical approximation satisfy three equations associated with each mesh point. These three equations each model the governing conservation law.

To begin with, we shall require that $u = u^*(x,t\,;j,n)$ satisfy the differential form of the conservation law, Eq. (1.1), within SE(j,n), i.e.,

$$(u_t)_j^n = -a\,(u_x)_j^n \tag{2.3}$$

We note in passing that, since u^* is a linear approximation, Eq. (2.3) can alternatively be arrived at by requiring u^* to satisfy the integral form of the conservation law, Eq. (1.3), within SE(j,n). Combining Eqs. (2.1) and (2.3), one has

$$u^*(x,t\,;j,n) = u_j^n + (u_x)_j^n\left[(x-x_j) - a\,(t-t^n)\right], \quad (x,t) \in \text{SE}(j,n). \tag{2.4}$$

From Eq. (1.4), $\vec{h} = (au,\, u)$. We therefore define

$$\vec{h}^*(x,t\,;j,n) \stackrel{\text{def}}{=} (au^*(x,t\,;j,n),\, u^*(x,t\,;j,n))\,. \tag{2.5}$$

Let E_2 be divided into nonoverlapping rectangular regions (see Fig. 3) referred to as conservation elements (CEs). As depicted in Figs. 5(a) and 5(b), the CE with its top-right (top-left) vertex being the mesh point $(j,n) \in \Omega_1$ is denoted by CE$_-(j,n)$ (CE$_+(j,n)$). Obviously the boundary of CE$_-(j,n)$ (CE$_+(j,n)$) is formed by subsets of SE(j,n) and SE$(j-1,n-1)$ (SE$(j+1,n-1)$). The numerical approximation u^* is now determined by requiring it to satisfy the integral conservation law applied to the CEs. This requirement yields the other two equations associated with each mesh point. The current approximation of Eq. (1.3) is

$$F_\pm(j,n) \stackrel{\text{def}}{=} \oint_{S(CE_\pm(j,n))} \vec{h}^* \cdot d\vec{s} = 0, \tag{2.6}$$

for all $(j,n) \in \Omega_1$. In other words, the total flux leaving the boundary of any CE is zero. Note that the flux at any interface separating two neighboring CEs is calculated using the information from a single SE. As an example, the interface AD depicted in Figs. 5(a) and 5(b) is a subset of SE(j,n). Thus the flux at this interface is calculated using the information associated with SE(j,n).

Because (i) The CEs associated with Ω_1 can fill any space-time region, and (ii) the surface integration across any interface separating two neighboring CEs is evaluated using the information from a single SE, the local conservation condition Eq. (2.6) leads to a global conservation relation, i.e., *the total flux leaving the boundary of any space-time region that is the union of any combination of CEs will also vanish.*

With the aid of Eqs. (2.4)–(2.6), it can be shown that (see [6, 4])

$$F_{\pm}(j,n)/\Delta x = \pm(1-\nu^2)\left[(u_x^+)_j^n + (u_x^+)_{j\pm1}^{n-1}\right] + (1\mp\nu)\left(u_j^n - u_{j\pm1}^{n-1}\right), \tag{2.7}$$

where $\nu = a\Delta t/\Delta x$ is the Courant number, and $(u_x^+)_j^n = (\Delta x/2)(u_x)_j^n$. Note that here Δx and Δt, respectively, represent the same mesh interval and time-step size which were denoted by $\Delta x/2$ and $\Delta t/2$ in [6, 4]. Eq. (2.6) or Eq. (2.7) represents two equations, one corresponding to the upper signs, and the other to the lower. This convention will also be used at other places in this report. Using Eqs. (2.6) and (2.7), u_j^n and $(u_x^+)_j^n$, which are considered as *independent* unknowns at the mesh point (j,n), can be solved for in terms of $u_{j\pm1}^{n-1}$ and $(u_x^+)_{j\pm1}^{n-1}$ if $1-\nu^2 \neq 0$. It is shown in [6, 4] that, for all $(j,n) \in \Omega_1$,

$$\vec{q}(j,n) = Q_+\,\vec{q}(j-1,\,n-1) + Q_-\,\vec{q}(j+1,\,n-1), \quad (1-\nu^2 \neq 0). \tag{2.8}$$

Here (i) $\vec{q}(j,n)$ is the column matrix formed by u_j^n and $(u_x^+)_j^n$, and (ii)

$$Q_{\pm} \stackrel{\text{def}}{=} (1/2)\begin{pmatrix} 1\pm\nu & \pm(1-\nu^2) \\ \mp 1 & -1\pm\nu \end{pmatrix}. \tag{2.9}$$

Eq. (2.8) defines a marching scheme. Because this scheme models Eq. (1.1) which is characterized by the parameter a, it is referred to as the a scheme. It is also shown in [6, 4] that the a scheme is stable provided that $\nu^2 < 1$, i.e., provided the CFL criterion is satisfied. Given u_j^n and $(u_x^+)_j^n$ at each point on a segment of some initial line of constant n, Eq. (2.8) may be used to find the numerical solution at points (j,n), at a later time. Because of the stability limit, such points must lie within the region of influence of the initial line segment. This stability requirement is reflective of the character of Eq. (1.1).

Because the local condition Eq. (2.3) explicitly allows us to easily eliminate $(u_t)_j^n$ in favor of $(u_x)_j^n$, the other flux conditions (2.7) are written in terms of u_j^n and $(u_x^+)_j^n$. Thus $(u_t)_j^n$ does not need to be stored, and u_j^n and $(u_x^+)_j^n$ can be considered to be the basic marching variables that are marched via Eq. (2.8).

The a scheme is in many ways an ideal solver for Eq. (1.1). The property of the a scheme of greatest significance for the construction of an implicit solver for Eq. (1.2) is its non-dissipative nature. The a scheme is the only *two-level explicit* solver of Eq. (1.1) known to the authors to be neutrally stable, i.e., free from numerical dissipation. It also has the simplest stencil, i.e., a triangle with a vertex at the given time level and the other two vertices at the previous time level. Because the flux at an interface separating two neighboring CEs is evaluated using information of a single SE, *no interpolation or extrapolation is required.* Moreover, the a scheme is a two-way marching scheme, i.e., a backward marching scheme in which $\vec{q}(j,n)$ *is determined in terms of* $\vec{q}(j-1,n+1)$ *and* $\vec{q}(j+1,n+1)$ can also be derived from Eq. (2.7). This is entirely in keeping with the invariance under time-reversal displayed by Eq. (1.1). The backward marching scheme may be used to find the numerical solution at points (j,n), at an earlier time. Such points must lie within the region of influence of a given initial line segment. These and other nontraditional features of the a scheme are discussed in depth in [6, 4].

In the above construction of the a scheme, we use the SEs and CEs of the mesh points marked by dots in Fig. 3 and Fig. 6. A similar construction can be performed by using the mesh points marked by triangles in Fig. 6. Let Ω_2 denote the set of mesh points (j,n) in E_2 (triangles in Fig. 6) where $n=0,\pm1,\pm2,\pm3,\ldots$, and, for each n, $j=n\pm1, n\pm3, n\pm5,\ldots$. Let the SEs and CEs of Ω_2 be defined by using Figs. 4 and 5(a)-(b), with dots replaced by triangles. Obviously (i) the CEs of Ω_2 also fill any space-time region, and (ii) the a scheme can also be constructed using the SEs and CEs of Ω_2. This new scheme is defined by Eq. (2.8) with $(j,n)\in\Omega_2$.

We remark on what may appear paradoxical about the overlapping of SEs and CEs associated with Ω_1 and Ω_2. Let $(j,n)\in\Omega_1$. Then (i) $(j+1,n)\in\Omega_2$, (ii) $\mathrm{SE}(j,n)$ and $\mathrm{SE}(j+1,n)$ overlap each other, and (iii) as depicted in Fig. 7, $\mathrm{CE}_+(j,n)$ and $\mathrm{CE}_-(j+1,n)$ represent the same rectangle in E_2. However, because the function $\vec{h}^*$ used in the evaluation of $F_+(j,n)$ is tied to a pair of SEs associated with Ω_1, while that used in the evaluation of $F_-(j+1,n)$ is tied to another pair of SEs associated with Ω_2, $F_+(j,n)=0$ and $F_-(j+1,n)=0$ represent *two completely independent flux conservation conditions.*

To prepare for the development of the implicit solvers to be described in the next section, we shall combine the above two independent schemes into a single scheme. The new scheme, referred to as the $a(2)$ scheme, is defined by Eq. (2.8) with $(j,n)\in\Omega$ where $\Omega\stackrel{\mathrm{def}}{=}\Omega_1\cup\Omega_2$. Obviously, a solution of the $a(2)$ scheme is formed by two decoupled solutions with each being associated with a mesh that is staggered in time. Several classical schemes also have this property. Among them are the Leapfrog, the DuFort-Frankel, and the Lax schemes [28]. We mention that the meshes Ω_1 and Ω_2 are duals of each other, in the sense used in the literature of finite-volume methods or of finite-element methods. We term their union the dual space-time mesh.

3 The implicit schemes

3.1 The a-$\mu(I1)$ scheme

An implicit solver for Eq. (1.2), referred to as the a-$\mu(I1)$ scheme, will be discussed in this sub-section. Here "I" stands for "implicit", and "1" is the identification number. This solver is the model for implicit time-dependent Navier-Stokes solvers under development. It is constructed to meet two requirements given in the following discussion:

(a) With a few exceptions, numerical dissipation generally appears in a numerical solution of a time-marching problem. In other words, the numerical solution dissipates faster than the corresponding physical solution. For a nearly inviscid problem, e.g., flow at a large Reynolds number, this could be a serious difficulty because numerical dissipation may overwhelm physical dissipation and cause a complete distortion of solutions. To avoid such a difficulty, the model solver is required to have the property that *the numerical dissipation shall approach zero as the physical dissipation approaches zero.*

(b) The convection term and the diffusion term in Eq. (1.2) involve the spatial derivatives of first order and second order, respectively. Thus, in a spatial region where a solution is very smooth, the diffusion term is negligible when compared with the convection term. As a result, the *effective* physical domain of dependence is more or less dictated by Eq. (1.1). To prevent excessive contamination of the solution by extraneous information, *the implicit solver shall be required to become an explicit solver in the limiting case in which the diffusion term vanishes.*

On the basis of the remarks (a) and (b), an implicit solver for Eq. (1.2) should reduce to an explicit nondissipative solver when $\mu = 0$. Because of these requirements, the implicit solver will be constructed such that it reduces to the $a(2)$ scheme if $\mu = 0$. The former differs from the latter only in the extra modeling involving the diffusion-related terms. Note that the presence of viscosity is felt through (i) the diffusion term $-\mu\partial^2 u/\partial x^2$ in Eq. (1.2), and (ii) the spatial diffusion flux component $-\mu\partial u/\partial x$ in the flux vector in Eq. (1.5).

We now construct the a-$\mu(I1)$ scheme, to numerically solve initial/boundary value problems involving Eq. (1.2). Let the initial and boundary values be given as

$$u(x,0) = u_I(x) \qquad \text{for } 0 \le x \le J\Delta x, \tag{3.1}$$

$$u(0,t) = u_L(t) \qquad \text{for } t > 0, \tag{3.2}$$

$$u(J\Delta x,t) = u_R(t) \qquad \text{for } t > 0, \tag{3.3}$$

where $u_I(x)$, $u_L(t)$, and $u_R(t)$ are given functions, and J and Δx are defined next. Consider the mesh depicted in Fig. 6 ($J \ge 4$), which is suitable for problems with stationary boundaries. There are J uniform spatial mesh intervals of size Δx. The temporal mesh intervals are each of size Δt. The SEs and CEs are defined in the interior as they are for the $a(2)$ scheme, which was described in the previous section. It follows that, for the current case, (i) Ω_1 and Ω_2 are restricted by the conditions $n \ge 0$ and $J \ge j \ge 0$, (ii) $\mathrm{CE}_{\pm}(j,n)$ are not defined if $n = 0$, (iii) $\mathrm{CE}_{-}(j,n)$ is not defined if $j = 0$, and (iv) $\mathrm{CE}_{+}(j,n)$ is not defined if $j = J$. Items (iii) and (iv) imply that *only one conservation condition is associated with a boundary mesh point.* Boundary values will supply the additional information needed to determine all discrete unknowns at a boundary mesh point. Obviously, the definition of $\mathrm{SE}(j,n)$ also needs to be appropriately modified if $j = 0$, or $j = J$, or $n = 0$.

We seek to determine an approximation u^* to the solution of the initial/boundary value problem. As in the $a(2)$ scheme, we specify that the approximant have a piecewise linear variation with space and time, i.e., Eq. (2.1) will still be assumed:

$$u^*(x,t\,;j,n) \stackrel{\text{def}}{=} u_j^n + (u_x)_j^n(x - x_j) + (u_t)_j^n(t - t^n) \quad , \qquad (x,t) \in \mathrm{SE}(j,n).$$

Numerical solution of the problem then reduces to determining the three unknown constants in Eq. (2.1) associated with each mesh point (j,n). At each boundary mesh point $(0,n)$ or (J,n), the applicable boundary condition will be used to determine two of the three unknowns. At each mesh point $(j,0)$ on the initial line, the initial condition will be used to

determine two of the three unknowns. Each of the corner points $(0,0)$ and $(J,0)$ is simultaneously a boundary point and a point on the initial line. At each of these corner points, all three constants in Eq. (2.1) are determined from the initial and boundary conditions.

Three equations, each representing a balance of space-time fluxes, will be developed at each interior mesh point (j,n). As in the a scheme, these equations will be numerical analogues of (a) the differential form of the conservation law evaluated at (j,n), (b) the integral form for $\mathrm{CE}_+(j,n)$, and (c) the integral form for $\mathrm{CE}_-(j,n)$. Also, one of (a), (b) and (c) will be written at each boundary or initial point which is not a corner point, thus providing a third condition at each such point in addition to the two conditions coming from initial or boundary values. Thus, the number of equations match the number of unknowns, with three equations and three unknowns being associated with each mesh point.

We proceed to develop the numerical analogue of the differential form of the conservation law at the point (j,n). We require the behavior of u^* to model Eq. (1.2). Simply substituting $u = u^*$ in Eq. (1.2), with u^* given by Eq. (2.1), would lead to Eq. (2.3) of the inviscid a scheme. Because the expansion in (2.1) is only linear, the second-derivative diffusion term in Eq. (1.2) is not modeled in Eq. (2.3). Instead, in the present scheme, we replace Eq. (2.3) with

$$(u_t)_j^n = -a(u_x)_j^n + \frac{\mu}{2\Delta x}\left[(u_x)_{j+1}^n - (u_x)_{j-1}^n\right], \quad J > j > 0, \tag{3.4}$$

for all $n \geq 0$. Eq. (3.4) is the numerical analogue of the differential condition Eq. (1.2). A comparison between Eqs. (1.2) and (3.4) reveals that *the diffusion term $-\mu\partial^2 u/\partial x^2$ at an interior mesh point $\in \Omega_1$ (Ω_2) is modeled by a central-difference approximation involving the values of u_x at two neighboring mesh points $\in \Omega_2$ (Ω_1)*. Note that Eqs. (2.1) and (3.4) imply that, for $J > j > 0$ and $(x,t) \in \mathrm{SE}(j,n)$,

$$\begin{aligned} & u^*(x,t\,;j,n) \\ = \; & u_j^n + (u_x)_j^n(x - x_j) + \left\{\frac{\mu}{2\Delta x}\left[(u_x)_{j+1}^n - (u_x)_{j-1}^n\right] - a(u_x)_j^n\right\}(t - t^n). \end{aligned} \tag{3.5}$$

Next, we develop the two remaining flux balance equations by requiring the numerical space-time fluxes to satisfy the integral form of the conservation law for the CEs defined in the previous section. To do this, first we form the numerical analogue of the flux vector defined by Eq. (1.5). Eq. (2.5) is replaced by

$$\vec{h}^*(x,t\,;j,n) \stackrel{\text{def}}{=} \left(au^*(x,t\,;j,n) - \mu u_x^*(x,t\,;j,n),\, u^*(x,t\,;j,n)\right), \tag{3.6}$$

for $(x,t) \in \mathrm{SE}(j,n)$. Here, the function u_x^* in the diffusive flux is defined as follows. For $(x,t) \in \mathrm{SE}(j,n)$,

$$u_x^*(x,t\,;j,n) \stackrel{\text{def}}{=} \begin{cases} w(u_x)_j^n + \overline{w}(u_x)_j^{n-1}, & \text{if } t \leq t^n; \\ \overline{w'}(u_x)_j^n + w'(u_x)_j^{n+1}, & \text{if } t > t^n. \end{cases} \tag{3.7}$$

where w and w' are weighting factors to be specified. The notations $\overline{w} \stackrel{\text{def}}{=} 1-w$ and $\overline{w'} \stackrel{\text{def}}{=} 1-w'$ have been used for compactness. Note that if $w' = w$, then $u_x^*(x,t\,;j,n-1) = u_x^*(x,t\,;j,n)$

in the region of overlap of SE(j,n) and SE$(j,n-1)$, i.e., in this case u_x^* is uniquely defined at any (x,t) where it is defined.

With the above modifications, the a-$\mu(I1)$ scheme is defined by assuming Eq. (2.6). Note that:

(a) At a mesh point $\in \Omega_1(\Omega_2)$, the diffusion-related terms in Eqs. (1.2) and (1.5) are modeled using *interpolations* that may involve the numerical values of the mesh points $\in \Omega_2(\Omega_1)$. *This contrasts sharply with the modeling of the convection-related terms which uses no interpolation.*

(b) In the $a(2)$ scheme, the two sets of numerical variables associated with the individual meshes Ω_1 and Ω_2 of the dual mesh are completely decoupled from each other. Contrarily, *they are glued together in the a-$\mu(I1)$ scheme through the interpolations referred to in (a).*

The conditions of flux conservation, Eq. (2.6) lead to the following equations, after integration and some algebra. Flux conservation for the element CE$_+(j,n)$, where the latter is defined, yields

$$\begin{aligned}
&\left[u_j^n + (u_x)_j^n \frac{\Delta x}{2}\right]\Delta x - \left[u_{j+1}^{n-1} - (u_x)_{j+1}^{n-1}\frac{\Delta x}{2}\right]\Delta x \\
&- \left\{a\left[u_j^n - (u_t)_j^n \frac{\Delta t}{2}\right] - \mu\left[w(u_x)_j^n + \overline{w}(u_x)_j^{n-1}\right]\right\}\Delta t \\
&+ \left\{a\left[u_{j+1}^{n-1} + (u_t)_{j+1}^{n-1}\frac{\Delta t}{2}\right] - \mu\left[w'(u_x)_{j+1}^n + \overline{w'}(u_x)_{j+1}^{n-1}\right]\right\}\Delta t \\
= \;& 0. \qquad (3.8)
\end{aligned}$$

Flux conservation for the element CE$_-(j,n)$, where the latter is defined, yields

$$\begin{aligned}
&\left[u_j^n - (u_x)_j^n \frac{\Delta x}{2}\right]\Delta x - \left[u_{j-1}^{n-1} + (u_x)_{j-1}^{n-1}\frac{\Delta x}{2}\right]\Delta x \\
&+ \left\{a\left[u_j^n - (u_t)_j^n \frac{\Delta t}{2}\right] - \mu\left[w(u_x)_j^n + \overline{w}(u_x)_j^{n-1}\right]\right\}\Delta t \\
&- \left\{a\left[u_{j-1}^{n-1} + (u_t)_{j-1}^{n-1}\frac{\Delta t}{2}\right] - \mu\left[w'(u_x)_{j-1}^n + \overline{w'}(u_x)_{j-1}^{n-1}\right]\right\}\Delta t \\
= \;& 0. \qquad (3.9)
\end{aligned}$$

It should be noted that during integration over the surface of CE$_+(j,n)$, only $\vec{h}^*(x,t\,;j,n)$ and $\vec{h}^*(x,t\,;j+1,n-1)$ are used, while for CE$_-(j,n)$, only $\vec{h}^*(x,t\,;j,n)$ and $\vec{h}^*(x,t\,;j-1,n-1)$ are used. Another point of interest is that the flux integration is made simple by the fact that the integral of a linearly varying flux over a straight line face of a CE is equal to the product of the length of the face and the value of the normal component of the flux at the midpoint of the face.

In the interests of compactness and clarity, symbols are now defined for groups of quantities occurring frequently in the discretized conservation equations. Let

$$\nu = a\frac{\Delta t}{\Delta x} \quad ; \quad \xi = 2\mu\frac{\Delta t}{\Delta x^2}; \qquad (3.10)$$

$$\left(u_x^+\right)_j^n = \frac{\Delta x}{2}\left(u_x\right)_j^n \qquad ; \qquad \left(u_t^+\right)_j^n = \frac{\Delta t}{2}\left(u_t\right)_j^n . \tag{3.11}$$

The magnitude of ν will be recognized as the Courant number, while ξ is a mesh-related diffusion parameter that arises in computations involving diffusion equations. Eq. (3.4) can be recast as

$$\left(u_t^+\right)_j^n = -\nu\left(u_x^+\right)_j^n + \frac{\xi}{4}\left[\left(u_x^+\right)_{j+1}^n - \left(u_x^+\right)_{j-1}^n\right] \tag{3.12}$$

for $J > j > 0$ and $n \geq 0$. Also, Eqs. (3.8) and (3.9) can be recast as

$$\begin{aligned} & \left[u_j^n + \left(u_x^+\right)_j^n\right] - \left[u_{j+1}^{n-1} - \left(u_x^+\right)_{j+1}^{n-1}\right] \\ & -\nu\left[u_j^n - \left(u_t^+\right)_j^n\right] + \xi\left[w(u_x^+)_j^n + \overline{w}(u_x^+)_j^{n-1}\right] \\ & +\nu\left[u_{j+1}^{n-1} + \left(u_t^+\right)_{j+1}^{n-1}\right] - \xi\left[w'(u_x^+)_{j+1}^n + \overline{w'}(u_x^+)_{j+1}^{n-1}\right] \\ = \; & 0, \qquad\qquad J > j \geq 0, \; n > 0, \end{aligned} \tag{3.13}$$

and

$$\begin{aligned} & \left[u_j^n - \left(u_x^+\right)_j^n\right] - \left[u_{j-1}^{n-1} + \left(u_x^+\right)_{j-1}^{n-1}\right] \\ & +\nu\left[u_j^n - \left(u_t^+\right)_j^n\right] - \xi\left[w(u_x^+)_j^n + \overline{w}(u_x^+)_j^{n-1}\right] \\ & -\nu\left[u_{j-1}^{n-1} + \left(u_t^+\right)_{j-1}^{n-1}\right] + \xi\left[w'(u_x^+)_{j-1}^n + \overline{w'}(u_x^+)_{j-1}^{n-1}\right] \\ = \; & 0, \qquad\qquad J \geq j > 0, \; n > 0. \end{aligned} \tag{3.14}$$

Collecting terms in Eqs. (3.13) and (3.14), we obtain

$$\begin{aligned} & (1-\nu)\,u_j^n + (1+w\xi)\left(u_x^+\right)_j^n - w'\xi\left(u_x^+\right)_{j+1}^n + \nu\left(u_t^+\right)_j^n \\ = \; & (1-\nu)\,u_{j+1}^{n-1} - \left(1-\overline{w'}\xi\right)\left(u_x^+\right)_{j+1}^{n-1} - \overline{w}\xi\left(u_x^+\right)_j^{n-1} - \nu\left(u_t^+\right)_{j+1}^{n-1} \end{aligned} \tag{3.15}$$

and

$$\begin{aligned} & (1+\nu)\,u_j^n - (1+w\xi)\left(u_x^+\right)_j^n + w'\xi\left(u_x^+\right)_{j-1}^n - \nu\left(u_t^+\right)_j^n \\ = \; & (1+\nu)\,u_{j-1}^{n-1} + \left(1-\overline{w'}\xi\right)\left(u_x^+\right)_{j-1}^{n-1} + \overline{w}\xi\left(u_x^+\right)_j^{n-1} + \nu\left(u_t^+\right)_{j-1}^{n-1} . \end{aligned} \tag{3.16}$$

We turn next to a consideration of the equations at the initial line and at the boundaries. Based upon the specification of the initial values, Eq. (3.1), we set

$$u_j^0 = u_I(x_j), \qquad 0 \leq j \leq J. \tag{3.17}$$

The initial-value information is also utilized to specify the spatial derivative on the initial line:

$$\left(u_x^+\right)_j^0 = \frac{\Delta x}{2}\frac{du_I}{dx}\left(x_j\right), \qquad 0 \leq j \leq J. \tag{3.18}$$

Similarly, based upon the specification of the boundary values, Eqs. (3.2) and (3.3), we set

$$u_0^n = u_L(t^n), \qquad n > 0, \tag{3.19}$$

$$u_J^n = u_R(t^n), \qquad n > 0. \tag{3.20}$$

The boundary information is also utilized to specify the temporal derivative on the boundary:

$$\left(u_t^+\right)_0^n = \frac{\Delta t}{2}\frac{du_L}{dt}(t^n), \qquad n \geq 0, \tag{3.21}$$

$$\left(u_t^+\right)_J^n = \frac{\Delta t}{2}\frac{du_R}{dt}(t^n), \qquad n \geq 0. \tag{3.22}$$

Eq. (3.12) and Eqs. (3.15)–(3.22) constitute three discretized equations per mesh point. On any line of constant n, $n \geq 0$, one equation at each mesh point is given by Eq. (3.12) for $0 < j < J$, by Eq. (3.21) for $j = 0$ and by Eq. (3.22) for $j = J$. These equations can be used to eliminate $\left(u_t^+\right)_j^n$ from the other two equations at each mesh point, as is done shortly. On the initial line $n = 0$, the two remaining discretized equations per mesh point are given by Eqs. (3.17) and (3.18). On any line of constant n, with $n > 0$, the two remaining equations associated with each mesh point are given by Eqs. (3.15) and (3.16) for $0 < j < J$, by Eqs. (3.15) and (3.19) for $j = 0$, and by Eqs. (3.16) and (3.20) for $j = J$.

We proceed to eliminate $\left(u_t^+\right)_j^n$ using one equation, from the other two equations at each mesh point, in order to express the latter equations in terms of only the marching variables u_j^n and $(u_x^+)_j^n$. At the boundaries, we will also substitute the boundary values given by Eqs. (3.19) and (3.20). It may be noted that the equations used to eliminate $\left(u_t^+\right)_j^n$, viz., Eqs. (3.12), (3.21) and (3.22), are applicable for any $n \geq 0$. Eqs. (3.17)–(3.20) do not involve a temporal derivative, thus leaving only Eqs. (3.15) and (3.16) to be transformed. When $1 \leq j \leq J-2$, we may substitute for $\left(u_t^+\right)_j^n$ and $\left(u_t^+\right)_{j+1}^{n-1}$ from Eq. (3.12) in Eq. (3.15) to obtain

$$\begin{aligned}
&(1-\nu)\,u_j^n - \frac{\nu\xi}{4}\left(u_x^+\right)_{j-1}^n + \left(1-\nu^2+w\xi\right)\left(u_x^+\right)_j^n + \left(\frac{\nu}{4}-w'\right)\xi\left(u_x^+\right)_{j+1}^n \\
= \;& (1-\nu)\,u_{j+1}^{n-1} - \frac{\nu\xi}{4}\left(u_x^+\right)_{j+2}^{n-1} - \left(1-\nu^2-\overline{w'}\xi\right)\left(u_x^+\right)_{j+1}^{n-1} \\
&+ \left(\frac{\nu}{4}-\overline{w}\right)\xi\left(u_x^+\right)_j^{n-1}, \qquad 1 \leq j \leq J-2.
\end{aligned} \tag{3.23}$$

When $2 \leq j \leq J-1$, we may substitute for $\left(u_t^+\right)_j^n$ and $\left(u_t^+\right)_{j+1}^{n-1}$ from Eq. (3.12) in Eq. (3.16) to obtain

$$\begin{aligned}
&(1+\nu)\,u_j^n - \frac{\nu\xi}{4}\left(u_x^+\right)_{j+1}^n - \left(1-\nu^2+w\xi\right)\left(u_x^+\right)_j^n + \left(\frac{\nu}{4}+w'\right)\xi\left(u_x^+\right)_{j-1}^n \\
= \;& (1+\nu)\,u_{j-1}^{n-1} - \frac{\nu\xi}{4}\left(u_x^+\right)_{j-2}^{n-1} + \left(1-\nu^2-\overline{w'}\xi\right)\left(u_x^+\right)_{j-1}^{n-1} \\
&+ \left(\frac{\nu}{4}+\overline{w}\right)\xi\left(u_x^+\right)_j^{n-1}, \qquad 2 \leq j \leq J-1.
\end{aligned} \tag{3.24}$$

When $2 \leq j \leq J-2$, Eqs. (3.23) and (3.24) will constitute the interior equations of the a-$\mu(I1)$ scheme.

At the left boundary $j = 0$, Eq. (3.19) is one equation associated with the mesh point. Substitution may be made in Eq. (3.15) for u_j^n from Eq. (3.19), for $(u_t^+)_j^n$ from Eq. (3.21), and for $\left(u_t^+\right)_{j+1}^{n-1}$ from Eq. (3.12). This gives

$$\begin{aligned} & (1-\nu)\, u_L(t^n) + (1+w\xi)\left(u_x^+\right)_j^n - w'\xi\left(u_x^+\right)_{j+1}^n + \nu\frac{\Delta t}{2}\frac{du_L}{dt}(t^n) \\ = \; & (1-\nu)\, u_{j+1}^{n-1} - \frac{\nu\xi}{4}\left(u_x^+\right)_{j+2}^{n-1} - \left(1-\nu^2-\overline{w'}\xi\right)\left(u_x^+\right)_{j+1}^{n-1} \\ & + \left(\frac{\nu}{4}-\overline{w}\right)\xi\left(u_x^+\right)_j^{n-1}, \qquad j=0, \end{aligned} \tag{3.25}$$

as the second associated equation.

At the adjoining mesh point $j = 1$, one of the associated equations is Eq. (3.23). Substitution may be made in Eq. (3.16) for $(u_t^+)_j^n$ from Eq. (3.12), for u_{j-1}^{n-1} from Eq. (3.19), and for $\left(u_t^+\right)_{j-1}^{n-1}$ from Eq. (3.21). This gives

$$\begin{aligned} & (1+\nu)\, u_j^n - \frac{\nu\xi}{4}\left(u_x^+\right)_{j+1}^n - \left(1-\nu^2+w\xi\right)\left(u_x^+\right)_j^n + \left(\frac{\nu}{4}+w'\right)\xi\left(u_x^+\right)_{j-1}^n \\ = \; & (1+\nu)\, u_L(t^{n-1}) + \left(1-\overline{w'}\xi\right)\left(u_x^+\right)_{j-1}^{n-1} + \overline{w}\xi\left(u_x^+\right)_j^{n-1} \\ & + \nu\frac{\Delta t}{2}\frac{du_L}{dt}\left(t^{n-1}\right), \qquad j=1, \end{aligned} \tag{3.26}$$

as the second associated equation.

At the other boundary mesh point $j = J$, one of the associated equations is Eq. (3.20). Substitution may be made in Eq. (3.16) for u_j^n from Eq. (3.20), for $(u_t^+)_j^n$ from Eq. (3.22), and for $\left(u_t^+\right)_{j-1}^{n-1}$ from Eq. (3.12). This gives

$$\begin{aligned} & (1+\nu)\, u_R(t^n) - (1+w\xi)\left(u_x^+\right)_j^n + w'\xi\left(u_x^+\right)_{j-1}^n - \nu\frac{\Delta t}{2}\frac{du_R}{dt}(t^n) \\ = \; & (1+\nu)\, u_{j-1}^{n-1} - \frac{\nu\xi}{4}\left(u_x^+\right)_{j-2}^{n-1} + \left(1-\nu^2-\overline{w'}\xi\right)\left(u_x^+\right)_{j-1}^{n-1} \\ & + \left(\frac{\nu}{4}+\overline{w}\right)\xi\left(u_x^+\right)_j^{n-1}, \qquad j=J, \end{aligned} \tag{3.27}$$

as the second associated equation.

Finally, at the adjoining mesh point $j = J-1$, one of the associated equations is Eq. (3.24). Substitution may be made in Eq. (3.15) for $(u_t^+)_j^n$ from Eq. (3.12), for u_{j+1}^{n-1} from Eq. (3.20), and for $\left(u_t^+\right)_{j+1}^{n-1}$ from Eq. (3.22). This gives

$$(1-\nu)\, u_j^n - \frac{\nu\xi}{4}\left(u_x^+\right)_{j-1}^n + \left(1-\nu^2+w\xi\right)\left(u_x^+\right)_j^n + \left(\frac{\nu}{4}-w'\right)\xi\left(u_x^+\right)_{j+1}^n$$

$$= (1-\nu)\,u_R(t^{n-1}) - \left(1-\overline{w'}\xi\right)\left(u_x^+\right)_{j+1}^{n-1} - \overline{w}\xi\left(u_x^+\right)_j^{n-1}$$
$$-\nu\frac{\Delta t}{2}\frac{du_R}{dt}\left(t^{n-1}\right), \qquad j = J-1, \tag{3.28}$$

as the second associated equation..

It should be noted that Eqs. (3.18), (3.21) and (3.22) assume differentiability of the functions u_I, u_L and u_R, respectively. This differentiability holds true for the numerical examples tested in this paper. However, a more general discretization of the initial and boundary conditions would be such that the discretized flux through the initial-line faces and the boundary faces of the CEs bordering the initial line and the boundaries equals the flux of the exact initial and boundary values, in an integral sense. For example, we would set

$$\left[u_j^0 - \left(u_x^+\right)_j^0\right]\Delta x = \int_{x_j-\Delta x}^{x_j} u_I(x)\,dx, \qquad 1 \le j \le J, \tag{3.29}$$

and

$$\left[u_j^0 + \left(u_x^+\right)_j^0\right]\Delta x = \int_{x_j}^{x_j+\Delta x} u_I(x)\,dx, \qquad 0 \le j \le J-1. \tag{3.30}$$

For $1 \le j \le J-1$, Eqs. (3.29) and (3.30), rather than Eqs. (3.17) and (3.18), would together determine u_j^0 and $(u_x^+)_j^0$. The values of u_0^0 and u_J^0 are obtained from Eq. (3.17), while $(u_x^+)_0^0$ is obtained from Eq. (3.30) and $(u_x^+)_J^0$ is obtained from Eq. (3.29). For the left boundary, we would set

$$\left[u_0^n - \left(u_t^+\right)_0^n\right]\Delta t = \int_{t^n-\Delta t}^{t^n} u_L(t)\,dt, \qquad n \ge 1, \tag{3.31}$$

and

$$\left[u_0^n + \left(u_t^+\right)_0^n\right]\Delta t = \int_{t^n}^{t^n+\Delta t} u_L(t)\,dt, \qquad n \ge 0. \tag{3.32}$$

For $n \ge 1$, Eqs. (3.31) and (3.32), rather than Eqs. (3.19) and (3.21), would together determine u_0^n and $\left(u_t^+\right)_0^n$. The value of $\left(u_t^+\right)_0^0$ is obtained from Eq. (3.32). The diffusive flux has not been accounted for in Eqs. (3.31) and (3.32), since it is not known from the exact boundary values. The right boundary values would be discretized in an analogous fashion. Such a general treatment would be valid even in the case in which the functions u_I, u_L and u_R may be discontinuous. This completes the discussion of the treatment of the boundary conditions.

Lastly, we express the interior equations, Eqs. (3.23) and (3.24), in matrix form with the aid of the following definitions

$$\overrightarrow{q}(j,n) \stackrel{def}{=} \begin{bmatrix} u_j^n \\ (u_x^+)_j^n \end{bmatrix} \tag{3.33}$$

$$Q_{-1}^{(1)} \stackrel{def}{=} \begin{pmatrix} 0 & -\nu\xi/4 \\ 0 & (\nu/4+w')\,\xi \end{pmatrix} \tag{3.34}$$

$$Q_0^{(1)} \stackrel{def}{=} \begin{pmatrix} 1-\nu & 1-\nu^2+w\xi \\ 1+\nu & -(1-\nu^2+w\xi) \end{pmatrix} \tag{3.35}$$

$$Q_1^{(1)} \stackrel{def}{=} \begin{pmatrix} 0 & (\nu/4 - w')\,\xi \\ 0 & -\nu\xi/4 \end{pmatrix} \tag{3.36}$$

$$Q_{-2}^{(2)} \stackrel{def}{=} \begin{pmatrix} 0 & 0 \\ 0 & -\nu\xi/4 \end{pmatrix} \tag{3.37}$$

$$Q_{-1}^{(2)} \stackrel{def}{=} \begin{pmatrix} 0 & 0 \\ 1+\nu & 1-\nu^2-\overline{w'}\xi \end{pmatrix} \tag{3.38}$$

$$Q_0^{(2)} \stackrel{def}{=} \begin{pmatrix} 0 & (\nu/4 - \overline{w})\,\xi \\ 0 & (\nu/4 + \overline{w})\,\xi \end{pmatrix} \tag{3.39}$$

$$Q_1^{(2)} \stackrel{def}{=} \begin{pmatrix} 1-\nu & -\left(1-\nu^2-\overline{w'}\xi\right) \\ 0 & 0 \end{pmatrix} \tag{3.40}$$

$$Q_2^{(2)} \stackrel{def}{=} \begin{pmatrix} 0 & -\nu\xi/4 \\ 0 & 0 \end{pmatrix} \tag{3.41}$$

With the preceding definitions, the interior Eqs. (3.23) and (3.24) may be expressed as

$$\begin{aligned} & Q_{-1}^{(1)}\overrightarrow{q}(j-1,n) + Q_0^{(1)}\overrightarrow{q}(j,n) + Q_1^{(1)}\overrightarrow{q}(j+1,n) \\ = \; & Q_{-2}^{(2)}\overrightarrow{q}(j-2,n-1) + Q_{-1}^{(2)}\overrightarrow{q}(j-1,n-1) + Q_0^{(2)}\overrightarrow{q}(j,n-1) \\ & + Q_1^{(2)}\overrightarrow{q}(j+1,n-1) + Q_2^{(2)}\overrightarrow{q}(j+2,n-1), \end{aligned}$$

i.e.,

$$\sum_{l=-1}^{1} Q_l^{(1)}\overrightarrow{q}(j+l,n) = \sum_{l=-2}^{2} Q_l^{(2)}\overrightarrow{q}(j+l,n-1). \tag{3.42}$$

3.2 The a-$\mu(I2)$ Scheme

This sub-section describes another implicit scheme, referred to as the a-$\mu(I2)$ scheme. In its specification, it differs from the a-$\mu(I1)$ scheme only in one respect, viz., Eq. (3.4) is replaced by

$$(u_t)_j^n = -a(u_x)_j^n + \frac{\mu}{(\Delta x)^2}(u_{j+1}^n + u_{j-1}^n - 2u_j^n), \qquad J > j > 1. \tag{3.43}$$

This involves an alternative representation of the diffusion term in the governing equation. The flux conservation conditions for CE_+ and CE_- are obtained as in the a-$\mu(I1)$ scheme, so that Eqs. (3.15) and (3.16) are also the other two equations associated with each interior mesh point in the a-$\mu(I2)$ scheme. However, the expression for the time derivative occurring in these equations is that arising from Eq. (3.43) rather than that from Eq. (3.4). It may be noted at this point that in two special cases, the a-$\mu(I1)$ and a-$\mu(I2)$ schemes become identical. The first case occurs when $\mu = 0$, when the viscous terms disappear, and the two implicit schemes become identical to each other and to the a scheme described in Section 2. The second case occurs when $a = 0$. In the latter case, $\nu = 0$, and the time derivative terms

occurring in Eqs. (3.15) and (3.16) vanish because of the factor ν. The two implicit schemes are then identical.

Eq. (3.43) can be recast as

$$(u_t^+)_j^n = -\nu(u_x)_j^n + \frac{\xi}{4}(u_{j+1}^n + u_{j-1}^n - 2u_j^n), \qquad J > j > 1 \tag{3.44}$$

On substituting for $\left(u_t^+\right)_j^n$ from Eq. (3.44) in Eqs. (3.15) and (3.16), we obtain the interior equations of the a-$\mu(I2)$ scheme:

$$\begin{aligned}
&\frac{\nu\xi}{4}u_{j-1}^n + \left(1 - \nu - \frac{\nu\xi}{2}\right)u_j^n + \frac{\nu\xi}{4}u_{j+1}^n \\
&+ \left(1 - \nu^2 + w\xi\right)\left(u_x^+\right)_j^n - w'\xi\left(u_x^+\right)_{j+1}^n \\
= \;& -\frac{\nu\xi}{4}u_{j+2}^{n-1} + \left(1 - \nu + \frac{\nu\xi}{2}\right)u_{j+1}^{n-1} - \frac{\nu\xi}{4}u_j^{n-1} \\
&- \left(1 - \nu^2 - \overline{w'}\xi\right)\left(u_x^+\right)_{j+1}^{n-1} - \overline{w}\xi\left(u_x^+\right)_j^{n-1}
\end{aligned} \tag{3.45}$$

and

$$\begin{aligned}
&-\frac{\nu\xi}{4}u_{j+1}^n + \left(1 + \nu + \frac{\nu\xi}{2}\right)u_j^n - \frac{\nu\xi}{4}u_{j-1}^n \\
&- \left(1 - \nu^2 + w\xi\right)\left(u_x^+\right)_j^n + w'\xi\left(u_x^+\right)_{j-1}^n \\
= \;& \frac{\nu\xi}{4}u_{j-2}^{n-1} + \left(1 + \nu - \frac{\nu\xi}{2}\right)u_{j-1}^{n-1} + \frac{\nu\xi}{4}u_j^{n-1} \\
&+ \left(1 - \nu^2 - \overline{w'}\xi\right)\left(u_x^+\right)_{j-1}^{n-1} + \overline{w}\xi\left(u_x^+\right)_j^{n-1}.
\end{aligned} \tag{3.46}$$

The boundary conditions are discretized in the same way as for the a-$\mu(I1)$ scheme, i.e., Eqs. (3.17) through (3.22) are assumed. The conservation equations at or adjoining the boundaries may by obtained from Eqs. (3.15) and (3.16) by substituting for $\left(u_t^+\right)_j^n$ from Eq. (3.44) or from the known boundary values, in a manner similar to that used in the a-$\mu(I1)$ scheme.

The interior equations (3.45) and (3.46) of the a-$\mu(I2)$ scheme may be expressed as Eq. (3.42), with the use of the following definitions:

$$Q_{-1}^{(1)} \stackrel{def}{=} \begin{pmatrix} \nu\xi/4 & 0 \\ -\nu\xi/4 & w'\xi \end{pmatrix} \tag{3.47}$$

$$Q_0^{(1)} \stackrel{def}{=} \begin{pmatrix} 1 - \nu - \nu\xi/2 & 1 - \nu^2 + w\xi \\ 1 + \nu + \nu\xi/2 & -(1 - \nu^2 + w\xi) \end{pmatrix} \tag{3.48}$$

$$Q_1^{(1)} \stackrel{def}{=} \begin{pmatrix} \nu\xi/4 & -w'\xi \\ -\nu\xi/4 & 0 \end{pmatrix} \tag{3.49}$$

$$Q_{-2}^{(2)} \stackrel{def}{=} \begin{pmatrix} 0 & 0 \\ \nu\xi/4 & 0 \end{pmatrix} \tag{3.50}$$

$$Q_{-1}^{(2)} \stackrel{def}{=} \begin{pmatrix} 0 & 0 \\ 1+\nu-\nu\xi/2 & 1-\nu^2-\overline{w'}\xi \end{pmatrix} \tag{3.51}$$

$$Q_{0}^{(2)} \stackrel{def}{=} \begin{pmatrix} -\nu\xi/4 & -\overline{w}\xi \\ \nu\xi/4 & \overline{w}\xi \end{pmatrix} \tag{3.52}$$

$$Q_{1}^{(2)} \stackrel{def}{=} \begin{pmatrix} 1-\nu+\nu\xi/2 & -\left(1-\nu^2-\overline{w'}\xi\right) \\ 0 & 0 \end{pmatrix} \tag{3.53}$$

$$Q_{2}^{(2)} \stackrel{def}{=} \begin{pmatrix} -\nu\xi/4 & 0 \\ 0 & 0 \end{pmatrix} \tag{3.54}$$

4 Solution Procedure

We will first discuss the solution procedure for the a-$\mu(I1)$ scheme. The $2(J+1)$ equations represented by Eqs. (3.19), (3.20) and (3.23)–(3.28) relate the $2(J+1)$ marching variables u_j^n and $(u_x^+)_j^n$ at the nth time level to the $2(J+1)$ marching variables u_j^{n-1} and $(u_x^+)_j^{n-1}$ at the $(n-1)$th time level. The equations thus define a time-marching scheme whereby the marching variables at the nth time level can be computed if the marching variables at the $(n-1)$th time level are known. Given values of the marching variables on the initial line, by Eqs. (3.17) and (3.18) for example, the scheme can be used to successively compute the marching variables at $n = 1, 2, 3, \ldots$. Next, we describe the solution of the implicit system of equations at any time level n.

The flux conservation relations associated with $\mathrm{CE}_+(j,n)$, namely, Eqs. (3.25), (3.23) and (3.28), can be rewritten as

(Eqs. (3.23) and (3.28))

$$\begin{aligned} & (1-\nu)\,u_j^n - \frac{\nu\xi}{4}\left(u_x^+\right)_{j-1}^n + \left(1-\nu^2+w\xi\right)\left(u_x^+\right)_j^n + \left(\frac{\nu}{4}-w'\right)\xi\left(u_x^+\right)_{j+1}^n \\ = \;& (S_+)_j^{n-1}, \qquad 1 \le j \le J-1 \end{aligned} \tag{4.1}$$

and (Eq. (3.25))

$$\begin{aligned} & (1+w\xi)\left(u_x^+\right)_j^n - w'\xi\left(u_x^+\right)_{j+1}^n \\ = \;& (S_+)_j^{n-1} - (1-\nu)\,u_L(t^n) - \nu\frac{\Delta t}{2}\frac{du_L}{dt}(t^n), \qquad j = 0, \end{aligned} \tag{4.2}$$

where

$$\begin{aligned} (S_+)_j^{n-1} = \;& (1-\nu)\,u_{j+1}^{n-1} - \frac{\nu\xi}{4}\left(u_x^+\right)_{j+2}^{n-1} - \left(1-\nu^2-\overline{w'}\xi\right)\left(u_x^+\right)_{j+1}^{n-1} \\ & + \left(\frac{\nu}{4}-\overline{w}\right)\xi\left(u_x^+\right)_j^{n-1}, \qquad 0 \le j \le J-2 \end{aligned} \tag{4.3}$$

and

$$(S_+)_j^{n-1} = (1-\nu)\,u_R\left(t^{n-1}\right) - \left(1-\overline{w'}\xi\right)\left(u_x^+\right)_{j+1}^{n-1} - \overline{w}\xi\left(u_x^+\right)_j^{n-1} - \nu\frac{\Delta t}{2}\frac{du_R}{dt}\left(t^{n-1}\right), \qquad j = J-1. \tag{4.4}$$

Similarly, the flux conservation relations associated with CE_(j,n), namely, Eqs. (3.26), (3.24) and (3.27), can be rewritten as

(Eqs. (3.26) and (3.24))

$$\begin{aligned}&(1+\nu)\,u_j^n - \frac{\nu\xi}{4}\left(u_x^+\right)_{j+1}^n - \left(1-\nu^2+w\xi\right)\left(u_x^+\right)_j^n + \left(\frac{\nu}{4}+w'\right)\xi\left(u_x^+\right)_{j-1}^n \\ &= (S_-)_j^{n-1}, \qquad 1 \le j \le J-1\end{aligned} \tag{4.5}$$

and (Eq. (3.27))

$$\begin{aligned}&-(1+w\xi)\left(u_x^+\right)_j^n + w'\xi\left(u_x^+\right)_{j-1}^n \\ &= (S_-)_j^{n-1} - (1+\nu)\,u_R\left(t^n\right) + \nu\frac{\Delta t}{2}\frac{du_R}{dt}\left(t^n\right), \qquad j = J,\end{aligned} \tag{4.6}$$

where

$$\begin{aligned}(S_-)_j^{n-1} &= (1+\nu)\,u_{j-1}^{n-1} - \frac{\nu\xi}{4}\left(u_x^+\right)_{j-2}^{n-1} + \left(1-\nu^2-\overline{w'}\xi\right)\left(u_x^+\right)_{j-1}^{n-1} \\ &\quad + \left(\frac{\nu}{4}+\overline{w}\right)\xi\left(u_x^+\right)_j^{n-1}, \qquad 2 \le j \le J\end{aligned} \tag{4.7}$$

and

$$(S_-)_j^{n-1} = (1+\nu)\,u_L\left(t^{n-1}\right) + \left(1-\overline{w'}\xi\right)\left(u_x^+\right)_{j-1}^{n-1} + \overline{w}\xi\left(u_x^+\right)_j^{n-1} + \nu\frac{\Delta t}{2}\frac{du_L}{dt}\left(t^{n-1}\right), \qquad j = 1. \tag{4.8}$$

In Eqs. (4.1), (4.2), (4.5) and (4.6), all terms which are known from either the $n-1$ time level or from the boundary conditions have been transferred to the right-hand side.

When $1 \le j \le J-1$, both Eq. (4.1) and (4.5) are applicable. Linear combinations of these equations imply that

$$\begin{aligned}&-\left[\frac{\nu}{2}+(1-\nu)w'\right]\xi\left(u_x^+\right)_{j-1}^n + 2\left(1-\nu^2+w\xi\right)\left(u_x^+\right)_j^n + \left[\frac{\nu}{2}-(1+\nu)w'\right]\xi\left(u_x^+\right)_{j+1}^n \\ &= (1+\nu)\,(S_+)_j^{n-1} - (1-\nu)\,(S_-)_j^{n-1}\end{aligned} \tag{4.9}$$

and

$$2u_j^n - w'\xi\left[\left(u_x^+\right)_{j+1}^n - \left(u_x^+\right)_{j-1}^n\right] = (S_+)_j^{n-1} + (S_-)_j^{n-1} \tag{4.10}$$

It may be noted that the u_j^n at the nth time level do not appear in Eq. (4.9). Note also that Eq. (4.10), obtained by adding corresponding sides of Eqs. (4.1) and (4.5), represents

flux conservation for the union of $\mathrm{CE}_+(j,n)$ and $\mathrm{CE}_-(j,n)$. Also, Eq. (4.10) implies that if $w' = 0$, then

$$u_j^n = \frac{1}{2}\left[(S_+)_j^{n-1} + (S_-)_j^{n-1}\right] \tag{4.11}$$

The equations (4.2), which is applicable at $j = 0$, (4.9), applicable for $1 \le j \le J-1$, and (4.6), applicable at $j = J$, together form a complete system of linear equations for the $(u_x^+)_j^n$ from which the u_j^n at the nth time level are absent or are known from boundary values. After the $(u_x^+)_j^n$ are computed by solving this system, the u_j^n in the interior can be found from Eq. (4.10). The u_j^n at the boundaries are known from Eqs. (3.19) and (3.20).

The system of equations for the unknowns $(u_x^+)_j^n$, $j = 0, \ldots, J$ is cast in matrix form with the aid of the following definitions :

$$\begin{aligned} &b_0 \stackrel{def}{=} 1 + w\xi \quad , \quad c_0 \stackrel{def}{=} -w'\xi \quad , \\ &d_0 \stackrel{def}{=} (S_+)_0^{n-1} - (1-\nu)\, u_L(t^n) - \nu \frac{\Delta t}{2} \frac{du_L}{dt}(t^n) \end{aligned} \tag{4.12}$$

$$\left.\begin{aligned} a_j &\stackrel{def}{=} -\left[\tfrac{\nu}{2} + (1-\nu)w'\right]\xi \\ b_j &\stackrel{def}{=} 2\left(1 - \nu^2 + w\xi\right) \\ c_j &\stackrel{def}{=} \left[\tfrac{\nu}{2} - (1+\nu)w'\right]\xi \\ d_j &\stackrel{def}{=} (1+\nu)\,(S_+)_j^{n-1} - (1-\nu)\,(S_-)_j^{n-1} \end{aligned}\right\} \quad j = 1, \ldots, J-1 \tag{4.13}$$

$$\begin{aligned} &a_J \stackrel{def}{=} w'\xi \quad , \quad b_J \stackrel{def}{=} -(1+w\xi) \quad , \\ &d_J \stackrel{def}{=} (S_-)_J^{n-1} - (1+\nu)\, u_R(t^n) + \nu \frac{\Delta t}{2} \frac{du_R}{dt}(t^n) \end{aligned} \tag{4.14}$$

$$v_j \stackrel{def}{=} \left(u_x^+\right)_j^n \quad , \quad j = 0, \ldots, J \tag{4.15}$$

The system may be written in matrix form as $\mathbf{A}\mathbf{v} = \mathbf{d}$, where $\mathbf{v}$ is a vector of length $J+1$ with ith entry v_i, $\mathbf{d}$ is a vector of length $J+1$ with ith entry d_i, and $\mathbf{A}$ is a $(J+1) \times (J+1)$ tridiagonal matrix with subdiagonal, leading diagonal and supradiagonal formed with the entries a_i, b_i and c_i respectively. Thus

$$A_{ij} = \begin{cases} a_i & \text{if } j = i-1 \\ b_i & \text{if } j = i \\ c_i & \text{if } j = i+1 \\ 0 & \text{otherwise} \end{cases} \tag{4.16}$$

It should be noted that the row and column indices of $\mathbf{A}$ and the row indices of $\mathbf{v}$ and $\mathbf{d}$ run from 0 to J.

We next show that the matrix $\mathbf{A}$ is diagonally dominant in rows and columns when certain conditions are met. Let

$$1 > \nu^2 \quad , \quad \xi \ge 0 \tag{4.17}$$

and

$$0.5 \leq w \leq 1 \quad , \quad w' = 1 - w \tag{4.18}$$

Then Eqs. (4.12)–(4.14), the definitions of the entries of matrix **A**, imply that

$$|b_0| = |b_J| = 1 + w\xi \quad , \quad |c_0| = |a_J| = (1-w)\xi \tag{4.19}$$

$$|b_j| = 2\left(1 - \nu^2 + w\xi\right) \tag{4.20}$$

$$|a_j| = \left|(1-w) + \frac{\nu}{2}(2w-1)\right|\xi \leq \left[(1-w) + \frac{|\nu|}{2}(2w-1)\right]\xi \tag{4.21}$$

$$|c_j| = \left|(1-w) - \frac{\nu}{2}(2w-1)\right|\xi \leq \left[(1-w) + \frac{|\nu|}{2}(2w-1)\right]\xi \tag{4.22}$$

where $j = 1, \ldots, J-1$. Thus

$$\begin{aligned} |b_j| - |a_j| - |c_j| &\geq 2\left[\left(1 - \nu^2 + w\xi\right) - (1-w)\xi - \frac{|\nu|}{2}(2w-1)\xi\right] \\ &= 2\left[1 - \nu^2 + (2w-1)\left(1 - \frac{|\nu|}{2}\right)\xi\right] > 0 \end{aligned} \tag{4.23}$$

where $j = 1, \ldots, J-1$. Obviously, we also have

$$|b_j| - |a_{j+1}| - |c_{j-1}| > 0 \quad , \quad j = 2, \ldots, J-2 \tag{4.24}$$

Also

$$|b_0| - |c_0| = |b_J| - |c_J| = 1 + (2w-1)\xi > 0 \tag{4.25}$$

$$\begin{aligned} |b_0| - |a_1| &\geq 1 + w\xi - \left[(1-w) + \frac{|\nu|}{2}(2w-1)\right]\xi \\ &= 1 + (2w-1)\left[1 - \frac{|\nu|}{2}\right]\xi > 0 \end{aligned} \tag{4.26}$$

$$\begin{aligned} |b_J| - |c_{J-1}| &\geq 1 + w\xi - \left[(1-w) + \frac{|\nu|}{2}(2w-1)\right]\xi \\ &= 1 + (2w-1)\left[1 - \frac{|\nu|}{2}\right]\xi > 0 \end{aligned} \tag{4.27}$$

$$\begin{aligned} |b_1| - |c_0| - |a_2| &\geq 2\left(1 - \nu^2 + w\xi\right) - (1-w)\xi - \left[(1-w) + \frac{|\nu|}{2}(2w-1)\right]\xi \\ &= 2\left[1 - \nu^2 + (2w-1)\left(1 - \frac{|\nu|}{4}\right)\xi\right] > 0 \end{aligned} \tag{4.28}$$

$$|b_{J-1}| - |c_{J-2}| - |a_J| \geq 2\left(1-\nu^2+w\xi\right) - (1-w)\xi - \left[(1-w) + \frac{|\nu|}{2}(2w-1)\right]\xi$$
$$= 2\left[1-\nu^2+(2w-1)\left(1-\frac{|\nu|}{4}\right)\xi\right] > 0 \qquad (4.29)$$

The above equations (4.19)–(4.29) imply that the $(J+1)\times(J+1)$ tridiagonal matrix $\mathbf{A}$ is strictly diagonally dominant in rows and columns. Thus the Thomas algorithm for solving the system is stable under the assumptions.

If Eq. (4.17) is assumed to be true, and the assumptions of Eq. (4.18) are replaced by

$$w \geq 1 \quad \text{and} \quad w' = 0 \qquad (4.30)$$

then the entries of the matrix $\mathbf{A}$ reduce to

$$|b_0| = |b_J| = 1 + w\xi \quad , \quad |a_J| = |c_0| = 0$$

$$|b_j| = 2\left(1-\nu^2+w\xi\right) \quad , \quad |a_j| = |c_j| = \frac{|\nu|}{2}\xi \quad , \quad j = 1,\ldots,J-1$$

From this, it can be shown that the matrix $\mathbf{A}$ is strictly diagonally dominant under the assumptions (4.30), and that the Thomas algorithm can therefore be used to perform the LU decomposition in a stable fashion.

The LU decomposition of the matrix $\mathbf{A}$ and solution of the system is performed via the Thomas algorithm as follows. Let

$$\beta_0 = b_0 \qquad (4.31)$$

$$\alpha_i = \frac{a_i}{\beta_{i-1}} \quad , \quad \beta_i = b_i - \alpha_i c_{i-1} \quad , \quad i = 1,\ldots,J \qquad (4.32)$$

This Gaussian elimination performs the LU decomposition of the matrix $\mathbf{A} = \mathbf{LU}$. The $(J+1)\times(J+1)$ bidiagonal matrix $\mathbf{L}$ has unity entries on the leading diagonal, and entries $\alpha_i\,(i=1,\ldots,J)$ on the subdiagonal, where i is the row index, which goes from 0 to J. The $(J+1)\times(J+1)$ bidiagonal matrix $\mathbf{U}$ has entries $\beta_i\,(i=0,\ldots,J)$ on the leading diagonal, and entries $c_i\,(i=0,\ldots,J-1)$ on the supradiagonal. The system $\mathbf{Av} = \mathbf{LUv} = \mathbf{d}$ is transformed to $\mathbf{Uv} = \mathbf{L}^{-1}\mathbf{d} = \boldsymbol{\delta}$ by a similar forward elimination process. The entries of $\boldsymbol{\delta}$ are

$$\delta_0 = d_0 \qquad (4.33)$$

$$\delta_i = d_i - \alpha_i d_{i-1} \quad , \quad i = 1,\ldots,J \qquad (4.34)$$

The system $\mathbf{Uv} = \boldsymbol{\delta}$ is then solved by a process of back-substitution

$$v_J = \frac{\delta_J}{\beta_J} \qquad (4.35)$$

and

$$v_i = \frac{1}{\beta_i}\left(\delta_i - c_i v_{i+1}\right) \quad , \quad i = J-1, \ldots, 0 \tag{4.36}$$

Finally, we mention that in the case of the a-$\mu(I2)$ scheme, prior elimination of the u_j^n at each mesh point to obtain a system for only the $(u_x^+)_j^n$ is not possible, as the conservation equations are implicit in both u_j^n and $(u_x)_j^n$. Hence, the resulting system for the u_j^n and the $(u_x^+)_j^n$ must be solved by a block version of the Thomas algorithm described above. This makes the a-$\mu(I1)$ scheme computationally more efficient than the a-$\mu(I2)$ scheme.

5 Stability Analysis

A rigorous discrete von Neumann stability analysis of the explicit 1D CE/SE schemes for scalar conservation laws was carried out in [1]. In this section, we use the stability analysis procedure to analyse the a-$\mu(I1)$ and a-$\mu(I2)$ schemes. For the rigorous development of the procedure, see [1].

We replace the discrete unknown with its discrete Fourier representation in the interior equation of the a-$\mu(I1)$ scheme, Eq. (3.42). Then we use linearity of the interior equation to isolate a single Fourier mode. This is equivalent to making the substitution

$$\vec{q}(j,n) = \vec{q}^*(n,\theta)\, e^{ij\theta} \qquad (i \equiv \sqrt{-1}, \quad -\pi < \theta \leq \pi) \tag{5.1}$$

in Eq. (3.42), where θ is the phase angle variation per unit Δx of a single Fourier mode. Performing this substitution, we obtain

$$Q^{(1)}(\nu,\xi,w,w',\theta)\, \vec{q}^*(n,\theta) = Q^{(2)}(\nu,\xi,w,w',\theta)\, \vec{q}^*(n-1,\theta), \tag{5.2}$$

where

$$\begin{aligned} & Q^{(1)}(\nu,\xi,w,w',\theta) \\ = & \sum_{l=-1}^{1} e^{li\theta} Q_l^{(1)} \\ = & \begin{bmatrix} 1-\nu & 1-\nu^2+w\xi - \frac{\nu\xi}{4}e^{-i\theta} + \xi\left(\frac{\nu}{4}-w'\right)e^{i\theta} \\ 1+\nu & -(1-\nu^2+w\xi) - \frac{\nu\xi}{4}e^{i\theta} + \xi\left(\frac{\nu}{4}-w'\right)e^{-i\theta} \end{bmatrix} \end{aligned} \tag{5.3}$$

and

$$\begin{aligned} & Q^{(2)}(\nu,\xi,w,w',\theta) \\ = & \sum_{l=-2}^{2} e^{li\theta} Q_l^{(2)} \\ = & \begin{bmatrix} (1-\nu)e^{i\theta} & -(1-\nu^2-(1-w')\,\xi)\,e^{i\theta} - \frac{\nu\xi}{4}e^{2i\theta} + \xi\left(\frac{\nu}{4}+w-1\right) \\ (1+\nu)e^{-i\theta} & (1-\nu^2-(1-w')\,\xi)\,e^{-i\theta} - \frac{\nu\xi}{4}e^{-2i\theta} + \xi\left(\frac{\nu}{4}+1-w\right) \end{bmatrix}. \end{aligned} \tag{5.4}$$

We examine the determinant of $Q^{(1)}$, to see when $Q^{(1)}$ is invertible. We have

$$\begin{aligned} & \Delta^{(1)}(\nu,\xi,w,w',\theta) \\ = \; & \det\left[Q^{(1)}(\nu,\xi,w,w',\theta)\right] \\ = \; & -2\left[\left(1-\nu^2\right)+\xi\left(w-w'\cos\theta\right)+i\left(\frac{1}{2}-w'\right)\nu\xi\sin\theta\right]. \end{aligned} \tag{5.5}$$

From the above equation, we note that $\Delta^{(1)} \neq 0$ for $-\pi < \theta \leq \pi$ if

$$\nu^2 < 1, \quad \xi \geq 0, \quad \text{and} \quad w \geq w'. \tag{5.6}$$

We assume that $\Delta^{(1)} \neq 0$. Then $\left[Q^{(1)}\right]^{-1}$ exists, and we can multiply Eq. (5.2) from the left by $\left[Q^{(1)}\right]^{-1}$, to define the amplification matrix

$$G(\nu,\xi,w,w',\theta) = \left[Q^{(1)}(\nu,\xi,w,w',\theta)\right]^{-1} Q^{(2)}(\nu,\xi,w,w',\theta). \tag{5.7}$$

An eigenvalue $\lambda(\nu,\xi,w,w',\theta)$ of $G(\nu,\xi,w,w',\theta)$ is defined by

$$G\vec{\phi} = \lambda\vec{\phi}$$

where $\vec{\phi}$ is the corresponding (non-zero) eigenvector of G. Multiplying from the left by $Q^{(1)}$, and using Eq. (5.7), we have

$$Q^{(2)}\vec{\phi} = \lambda Q^{(1)}\vec{\phi}. \tag{5.8}$$

Thus, any eigenvalue $\lambda(\nu,\xi,w,w',\theta)$ of $G(\nu,\xi,w,w',\theta)$ satisfies the condition

$$\det\left[Q^{(2)}(\nu,\xi,w,w',\theta) - \lambda Q^{(1)}(\nu,\xi,w,w',\theta)\right] = 0. \tag{5.9}$$

Using the definitions Eqs. (5.3) and (5.4), Eq. (5.9) is equivalent to

$$A\lambda^2 + B\lambda + C = 0, \tag{5.10}$$

where

$$A = \left(1-\nu^2\right)+\xi\left(w-w'\cos\theta\right)+i\left(\frac{1}{2}-w'\right)\nu\xi\sin\theta, \tag{5.11}$$

$$\begin{aligned} B \; = \; & \xi\left[1-\cos\theta+(w'-w)\left(1+\cos\theta\right)-\nu^2\sin^2\theta\right] \\ & +i\nu\left[2\left(1-\nu^2\right)+\left(w+w'-1\right)\xi\right]\sin\theta \end{aligned} \tag{5.12}$$

and

$$C = -\left(1-\nu^2\right)+\xi\left[1-w'-(1-w)\cos\theta\right]+i\left(\frac{1}{2}-w\right)\nu\xi\sin\theta. \tag{5.13}$$

Thus, the eigenvalues of amplification matrix are given by

$$\lambda_{\pm} = \frac{-B \pm \sqrt{B^2-4AC}}{2A}. \tag{5.14}$$

These eigenvalues constitute the two amplification factors of the a-$\mu(I1)$ scheme. Note that there are two amplification factors rather than one, because there are two unknowns at each mesh point. Let $\theta = 0$. Then we find from Eqs. (5.20)-(5.14) that

$$\lambda_+ = 1, \quad \text{and} \quad \lambda_- = \frac{(w - w')\,\xi - (1 - \nu^2)}{(w - w')\,\xi + (1 - \nu^2)} \qquad (\text{when } \theta = 0).$$

Substituting $\theta = 0$ in Eqs. (5.3) and (5.4), and using the results in Eq. (5.8), we obtain

$$\begin{bmatrix} 0 & -2\,(1 - \nu^2) \\ 0 & 2\,(1 - \nu^2) \end{bmatrix} \vec{\phi} = \mathbf{0},$$

whence we find that the eigenvector of G corresponding to $\lambda_+ = 1$ is given by

$$\vec{\phi}(\theta = 0,\ \lambda = 1) = \alpha \begin{bmatrix} 1 \\ 0 \end{bmatrix}$$

where α is an arbitrary constant. Based upon these facts, we term λ_+ the principal amplification factor, because it is exhibits the principal effect of the scheme on a wave of zero frequency. λ_- is termed the spurious amplification factor.

For general θ, the behavior of the amplification factors must be investigated numerically. Numerical experiments show that if either (i) $0.5 \leq w \leq 1$ and $w' = 1 - w$, or (ii) $w > 1$ and (w, w') lies between the lines $w + w' = 1$ and $w - w' = 1$ in the (w, w') plane, then the a-$\mu(I1)$ scheme is stable provided

$$\nu^2 < 1 \qquad \text{and} \qquad \xi \geq 0. \tag{5.15}$$

This condition on the stability applies, in particular, to the special case $w = w' = 1/2$.

Note that many other implicit solvers are unconditionally stable. However, the price paid for this "desirable" property usually is excessive numerical dissipation. Moreover, the use of a time-step size that is greater than that allowed by Eq. (5.15) generally results in a less accurate time-dependent solution. Thus we do not consider the more restrictive stability condition Eq. (5.15) to be a disadvantage of the a-$\mu(I1)$ scheme.

We turn now to a closer examination of the amplification factors for the special case $w = w' = 1/2$. In Section 6, where the consistency and truncation error of the current implicit schemes are considered, it is shown that in this case, the a-$\mu(I1)$ scheme is second-order accurate in space and time. In this case, Eqs. (5.20)-(5.22) become

$$A = 1 - \nu^2 + \frac{\xi}{2}\,(1 - \cos\theta) \qquad (w = w' = 1/2)$$

$$B = \xi\left[1 - \cos\theta - \nu^2 \sin^2\theta\right] + 2i\nu(1 - \nu^2)\sin\theta \qquad (w = w' = 1/2)$$

$$C = -\left(1 - \nu^2\right) + \frac{\xi}{2}\,(1 - \cos\theta) \qquad (w = w' = 1/2)$$

Then, corresponding to Eq. (5.10), we have

$$\lambda_{\pm} = \frac{-Q \pm \sqrt{Q^2 + (1-\nu^2)^2 - \xi^2 (1-\cos\theta)^2 / 4}}{1 - \nu^2 + \xi (1 - \cos\theta)} \tag{5.16}$$

where

$$Q = \frac{\xi}{2}\left(1 - \cos\theta - \nu^2 \sin^2\theta\right) + i\nu(1-\nu^2)\sin\theta.$$

In particular, when $a = 0$, i.e., when the scheme becomes a second-order accurate solver for the pure diffusion equation, then $\nu = 0$, and Eq. (5.16) can be simplified to yield

$$\lambda_+ = \frac{1 - \xi \sin^2(\theta/2)}{1 + \xi \sin^2(\theta/2)}, \qquad \lambda_- = -1 \qquad (w = w' = 1/2,\ \nu = 0)$$

It is found that λ_+ is identical to the amplification factor of the Crank-Nicolson scheme ([28], p. 112).

We next analyse the stability of the a-$\mu(I2)$ scheme, with the same procedure as was used for the a-$\mu(I1)$ scheme. The substitution (5.1) in Eq. (3.42), with the definitions (3.47)–(3.54), lead to Eq. (5.2), where

$$\begin{aligned} & Q^{(1)}(\nu, \xi, w, w', \theta) \\ = & \sum_{l=-1}^{1} e^{li\theta} Q_l^{(1)} \\ = & \begin{bmatrix} \frac{\nu\xi}{2}\cos\theta + 1 - \nu - \frac{\nu\xi}{2} & 1 - \nu^2 + w\xi - w'\xi e^{i\theta} \\ -\frac{\nu\xi}{2}\cos\theta + 1 + \nu + \frac{\nu\xi}{2} & -(1 - \nu^2 + w\xi) + w'\xi e^{-i\theta} \end{bmatrix} \end{aligned} \tag{5.17}$$

and

$$\begin{aligned} & Q^{(2)}(\nu, \xi, w, w', \theta) \\ = & \sum_{l=-2}^{2} e^{li\theta} Q_l^{(2)} \\ = & \begin{bmatrix} -\frac{\nu\xi}{4} + (1 - \nu + \frac{\nu\xi}{2})e^{i\theta} - \frac{\nu\xi}{4}e^{2i\theta} & -(1 - \nu^2 - (1-w')\,\xi)\,e^{i\theta} - (1-w)\,\xi \\ \frac{\nu\xi}{4} + (1 + \nu - \frac{\nu\xi}{2})e^{-i\theta} + \frac{\nu\xi}{4}e^{-2i\theta} & (1 - \nu^2 - (1-w')\,\xi)\,e^{-i\theta} + (1-w)\,\xi \end{bmatrix} \end{aligned} \tag{5.18}$$

We examine the determinant of $Q^{(1)}$, to see when $Q^{(1)}$ is invertible. We have

$$\begin{aligned} & \Delta^{(1)}(\nu, \xi, w, w', \theta) \\ = & \det\left[Q^{(1)}(\nu, \xi, w, w', \theta)\right] \\ = & -2\left[\left(1 - \nu^2\right) + \xi\,(w - w'\cos\theta) - i\left(1 + \xi\sin^2\left(\frac{\theta}{2}\right)\right) w'\nu\xi\sin\theta\right]. \end{aligned} \tag{5.19}$$

As in the case of the a-$\mu(I1)$ scheme, we find that $\Delta^{(1)} \neq 0$ for $-\pi < \theta \leq \pi$ if Eq. (5.6) is satisfied.

We assume that $\Delta^{(1)} \neq 0$. Following the same logic as in the case of the a-$\mu(I1)$ scheme, we find that the eigenvalues of the amplification matrix for the a-$\mu(I2)$ scheme satisfy Eq. (5.9). This can be solved to yield the eigenvalues, as in Eq. (5.14), where Eqs. (5.20)–(5.22) are replaced by

$$A = \left(1-\nu^2\right) + \xi\left(w - w'\cos\theta\right) - i\left(1 + \xi\sin^2\left(\frac{\theta}{2}\right)\right) w'\nu\xi\sin\theta, \tag{5.20}$$

$$\begin{aligned} B &= \xi\left[1-\cos\theta + (w'-w)\left(1+\cos\theta\right)\right] \\ &\quad + i\nu\left[2\left(1-\nu^2\right) + (w+w'-1)\,\xi - \frac{\xi^2}{2}\left(1+w-w'\right)\left(1-\cos\theta\right)\right]\sin\theta \end{aligned} \tag{5.21}$$

and

$$C = -\left(1-\nu^2\right) + \xi\left[1-w'-(1-w)\cos\theta\right] + i\left(1-\xi\sin^2\left(\frac{\theta}{2}\right)\right)(1-w)\nu\xi\sin\theta. \tag{5.22}$$

Numerical evaluation of the amplification factors of the a-$\mu(I2)$ scheme, shows that when (i) $w \geq 0.5$ and (ii) $w' = w$, the scheme is stable when Eq. (5.15) is satisfied. As pointed out in Section 3, when $\nu = 0$, the a-$\mu(I1)$ scheme and the a-$\mu(I2)$ scheme become identical. Hence, the a-$\mu(I2)$ scheme shares with the a-$\mu(I1)$ scheme the property that when $\nu = 0$, its principal amplification factor becomes identical to the amplification factor of the Crank-Nicolson scheme.

6 Consistency and Truncation Error

In this section, we discuss the consistency and truncation error of, successively, the a-$\mu(I1)$ scheme and the a-$\mu(I2)$ scheme. It will be indicated that, under certain conditions, the interior discretized equations of the schemes are consistent with a pair of partial differential equations (PDEs). One of these PDEs is Eq. (1.2). In the following analysis, the grid point values of continuous functions of space and time are denoted by using grid indices as superscripts and subscripts.

The flux conservation relation Eq. (3.24) is written for CE$_-(j+1,n)$. This is symbolized by

$$F_-(j+1,n) = 0 \tag{6.1}$$

Eqs. (3.23) and (6.1) are two distinct conservation equations, although the conservation elements involved occupy the same physical region. The a-$\mu(I1)$ scheme can obviously alternatively be described by specifying these two equations. Linear combinations of these equations are next examined, in order to investigate the consistency of the scheme. Adding Eq. (3.23) and Eq. (6.1), and dividing throughout by $2\,\triangle x\,\triangle t$, results in

$$\left[FDE1(u,u_x)\right]_{j+\frac{1}{2}}^{n-\frac{1}{2}} = 0 \tag{6.2}$$

with $FDE1$ as defined below. Also, subtracting Eq. (6.1) from Eq. (3.23), and dividing throughout by $2(1-\nu^2)\,\triangle x^2$, results in

$$[FDE2(u,u_x)]_{j+\frac{1}{2}}^{n-\frac{1}{2}} = 0 \tag{6.3}$$

Here, $FDE1$ and $FDE2$ are defined as

$$\begin{aligned}
&[FDE1(u,v)]_{j+\frac{1}{2}}^{n-\frac{1}{2}} \stackrel{def}{=} \\
&\frac{1}{2\,\triangle t}\left[u_{j+1}^{n}-u_{j+1}^{n-1}+u_{j}^{n}-u_{j}^{n-1}\right]+\frac{a}{2\,\triangle x}\left[u_{j+1}^{n}-u_{j}^{n}+u_{j+1}^{n-1}-u_{j}^{n-1}\right] \\
&-\frac{\mu}{2\,\triangle x}\left[v_{j+1}^{n}-v_{j}^{n}+v_{j+1}^{n-1}-v_{j}^{n-1}\right] \\
&-\left[\frac{\mu\,(w'+w-1)}{2\,\triangle x}+\frac{\triangle x}{4\,\triangle t}-\frac{\nu a}{4}\right]\left[v_{j+1}^{n}-v_{j}^{n}-v_{j+1}^{n-1}+v_{j}^{n-1}\right] \\
&+\frac{\nu\mu}{8\,\triangle x}\left[v_{j+2}^{n-1}-v_{j}^{n-1}+v_{j+1}^{n}-v_{j-1}^{n}-v_{j+2}^{n}+v_{j}^{n}-v_{j+1}^{n-1}+v_{j-1}^{n-1}\right]
\end{aligned} \tag{6.4}$$

$$\begin{aligned}
&[FDE2(u,v)]_{j+\frac{1}{2}}^{n-\frac{1}{2}} \stackrel{def}{=} \\
&\frac{1}{4}\left[v_{j+1}^{n}+v_{j}^{n}+v_{j+1}^{n-1}+v_{j}^{n-1}\right] \\
&+\frac{\nu\xi}{8\,(1-\nu^2)}\left[v_{j+2}^{n}-v_{j}^{n}+v_{j+1}^{n}-v_{j-1}^{n}+v_{j+2}^{n-1}-v_{j}^{n-1}+v_{j+1}^{n-1}-v_{j-1}^{n-1}\right] \\
&-\frac{1}{2\,(1-\nu^2)\,\triangle x}\left[u_{j+1}^{n}-u_{j}^{n}+u_{j+1}^{n-1}-u_{j}^{n-1}\right] \\
&-\frac{\nu}{2\,(1-\nu^2)\,\triangle x}\left[u_{j+1}^{n}-u_{j+1}^{n-1}+u_{j}^{n}-u_{j}^{n-1}\right] \\
&-\frac{\xi\,(w-w')}{2\,(1-\nu^2)}\left[v_{j+1}^{n}-v_{j+1}^{n-1}+v_{j}^{n}-v_{j}^{n-1}\right]
\end{aligned} \tag{6.5}$$

Let $\tilde{u}(x,t)$ and $\tilde{v}(x,t)$ be smooth functions, and let

$$\tilde{p} \stackrel{def}{=} \tilde{v} - \frac{\partial \tilde{u}}{\partial x} \tag{6.6}$$

Define, further, partial differential expressions $PDE1$ and $PDE2$ by

$$PDE1(u) \stackrel{def}{=} \frac{\partial u}{\partial t} + a\frac{\partial u}{\partial x} - \mu\frac{\partial^2 u}{\partial x^2} \tag{6.7}$$

$$PDE2(p) \stackrel{def}{=} p + \frac{\nu\xi\,\triangle x}{1-\nu^2}\frac{\partial p}{\partial x} \tag{6.8}$$

$[FDE1(\tilde{u},\tilde{v})]_{j+\frac{1}{2}}^{n-\frac{1}{2}}$ and $[FDE2(\tilde{u},\tilde{v})]_{j+\frac{1}{2}}^{n-\frac{1}{2}}$ may be considered to be discrete approximations to $[PDE1(\tilde{u})]_{j+\frac{1}{2}}^{n-\frac{1}{2}}$ and $[PDE2(\tilde{p})]_{j+\frac{1}{2}}^{n-\frac{1}{2}}$, respectively. Then the errors $ER1$ and $ER2$ in these

approximations are defined by

$$[ER1]_{j+\frac{1}{2}}^{n-\frac{1}{2}} \stackrel{def}{=} [FDE1(\tilde{u},\tilde{v})]_{j+\frac{1}{2}}^{n-\frac{1}{2}} - [PDE1(\tilde{u})]_{j+\frac{1}{2}}^{n-\frac{1}{2}} \tag{6.9}$$

$$[ER2]_{j+\frac{1}{2}}^{n-\frac{1}{2}} \stackrel{def}{=} [FDE2(\tilde{u},\tilde{v})]_{j+\frac{1}{2}}^{n-\frac{1}{2}} - [PDE2(\tilde{p})]_{j+\frac{1}{2}}^{n-\frac{1}{2}} \tag{6.10}$$

With the aid of Taylor expansions, it may be shown that

$$\begin{aligned}
[ER1]_{j+\frac{1}{2}}^{n-\frac{1}{2}} &= -\mu\frac{\partial\tilde{p}}{\partial x} - \mu\left(w'+w-1\right)\frac{\partial^2\tilde{v}}{\partial x\,\partial t}\triangle t + \frac{\partial^3\tilde{u}}{\partial x^2\partial t}\frac{\triangle x^2}{8} + \frac{\partial^3\tilde{u}}{\partial t^3}\frac{\triangle t^2}{24} \\
&\quad + a\frac{\partial^3\tilde{u}}{\partial x^3}\frac{\triangle x^2}{24} + a\frac{\partial^3\tilde{u}}{\partial x\,\partial t^2}\frac{\triangle t^2}{8} - \mu\frac{\partial^3\tilde{v}}{\partial x^3}\frac{\triangle x^2}{24} - \mu\frac{\partial^3\tilde{v}}{\partial x\,\partial t^2}\frac{\triangle t^2}{8} \\
&\quad + \frac{1}{8}\frac{\partial^2\tilde{v}}{\partial x\,\partial t}\left[a^2\triangle t^2 - \triangle x^2\right] - a\mu\frac{\partial^3\tilde{v}}{\partial x^2\partial t}\frac{\triangle t^2}{4} + O\left(\triangle^3\right)
\end{aligned} \tag{6.11}$$

It may similarly be shown that

$$\begin{aligned}
&[ER2]_{j+\frac{1}{2}}^{n-\frac{1}{2}} \\
&= \frac{-\nu\,\triangle t}{\left(1-\nu^2\right)\triangle x}\left[\frac{\partial\tilde{u}}{\partial t} + a\frac{\partial\tilde{u}}{\partial x} - \mu\frac{\partial^2\tilde{u}}{\partial x^2}\right] - \frac{\xi\left(w-w'\right)}{\left(1-\nu^2\right)}\frac{\partial\tilde{v}}{\partial t}\triangle t \\
&\quad - \frac{\xi\left(w-w'\right)}{\left(1-\nu^2\right)}O\left(\triangle^3\right) + \frac{\partial^2\tilde{v}}{\partial x^2}\frac{\triangle x^2}{8} + \frac{\partial^2\tilde{v}}{\partial t^2}\frac{\triangle t^2}{8} \\
&\quad + \frac{\nu\xi\,\triangle x}{24\left(1-\nu^2\right)}\left[7\frac{\partial^3\tilde{v}}{\partial x^3}\triangle x^2 + 3\frac{\partial^3\tilde{v}}{\partial x\,\partial t^2}\triangle t^2\right] \\
&\quad - \frac{1}{24\left(1-\nu^2\right)}\left[\frac{\partial^3\tilde{u}}{\partial x^3}\triangle x^2 + 3\frac{\partial^3\tilde{u}}{\partial x\,\partial t^2}\triangle t^2\right] \\
&\quad - \frac{\nu\,\triangle t}{24\left(1-\nu^2\right)\triangle x}\left[3\frac{\partial^3\tilde{u}}{\partial x^2\partial t}\triangle x^2 + \frac{\partial^3\tilde{u}}{\partial t^3}\triangle t^2\right] + O\left(\triangle^3\right) \\
&\quad + \frac{\nu\xi\,\triangle x}{\left(1-\nu^2\right)}O\left(\triangle^3\right) - \frac{1}{\left(1-\nu^2\right)}O\left(\triangle^3\right) - \frac{\nu\,\triangle t}{\left(1-\nu^2\right)\triangle x}O\left(\triangle^3\right)
\end{aligned} \tag{6.12}$$

In Eqs. (6.11) and (6.12), all derivatives are evaluated at $((j+1/2)\,\triangle x, (n-1/2)\,\triangle t)$. Each symbol $O\left(\triangle^3\right)$ represents an infinite sum of terms, in which derivatives of $\tilde{u}$ or $\tilde{v}$, and the quantities a, μ and $\triangle x^l \triangle t^m$ occur only as factors in the numerator of each term, with $l, m \geq 0$ and $l+m \geq 3$.

Let $\tilde{u}$ and $\tilde{v}$ be a solution of the system of PDEs formed by $PDE1(\tilde{u}) = 0$ and $\tilde{p} = 0$. Then $[FDE1(\tilde{u},\tilde{v})]_{j+\frac{1}{2}}^{n-\frac{1}{2}}$ and $[FDE2(\tilde{u},\tilde{v})]_{j+\frac{1}{2}}^{n-\frac{1}{2}}$ are by definition the truncation errors of the discrete equations (6.2) and (6.3) satisfied by a solution of the a-$\mu(I1)$ scheme. Also, now $[PDE1(\tilde{u})]_{j+\frac{1}{2}}^{n-\frac{1}{2}} = 0$ and $[PDE2(\tilde{p})]_{j+\frac{1}{2}}^{n-\frac{1}{2}} = 0$. Hence, $[FDE1(\tilde{u},\tilde{v})]_{j+\frac{1}{2}}^{n-\frac{1}{2}} = [ER1]_{j+\frac{1}{2}}^{n-\frac{1}{2}}$ and $[FDE2(\tilde{u},\tilde{v})]_{j+\frac{1}{2}}^{n-\frac{1}{2}} = [ER2]_{j+\frac{1}{2}}^{n-\frac{1}{2}}$. Also, the first term on the right hand side of each of Eqs. (6.11) and (6.12) is zero. Assume $\nu^2 \neq 1$. Let the rule of mesh refinement be such that

$\frac{\triangle t}{\triangle x}$ remains bounded as $\triangle x \to 0$ and $\triangle t \to 0$. This implies that ν and $\xi \triangle x$ also remain bounded. Examination of $ER1$ and $ER2$ shows that the discrete equations (6.2) and (6.3) are in general consistent with only the stationary forms of $PDE1(\tilde{u}) = 0$ and $PDE2(\tilde{p}) = 0$. The second term on the right hand side of Eq. (6.12) represents a time-inconsistency, which makes the scheme only first-order accurate for u_j^n. If $w = w'$, the a-$\mu(I1)$ scheme is time-consistent, but is in general only first-order accurate in time because of the second term on the right hand side of Eq. (6.11). If, additionally, $w + w' = 1$, i.e. $w = w' = 1/2$, then the discrete equations of the a-$\mu(I1)$ scheme are consistent with $PDE1(\tilde{u}) = 0$ and $PDE2(\tilde{p}) = 0$, and the scheme is second-order accurate in space and time.

We turn next to a similar analysis of the a-$\mu(I2)$ scheme. Manipulations similar to those leading to Eqs. (6.2) and (6.3) are performed on the interior equations (3.45) and (3.46) of the a-$\mu(I2)$ scheme. This yields the equations

$$[FDE3(u, u_x)]_{j+\frac{1}{2}}^{n-\frac{1}{2}} = 0 \tag{6.13}$$

$$[FDE4(u, u_x)]_{j+\frac{1}{2}}^{n-\frac{1}{2}} = 0 \tag{6.14}$$

Here $FDE3$ and $FDE4$ are defined as

$$\begin{aligned}
&[FDE3(u,v)]_{j+\frac{1}{2}}^{n-\frac{1}{2}} \stackrel{def}{=} \\
&\frac{1}{2\triangle t}\left[u_{j+1}^n - u_{j+1}^{n-1} + u_j^n - u_j^{n-1}\right] + \frac{a}{2\triangle x}\left[u_{j+1}^n - u_j^n + u_{j+1}^{n-1} - u_j^{n-1}\right] \\
&-\frac{\mu}{2\triangle x}\left[v_{j+1}^n - v_j^n + v_{j+1}^{n-1} - v_j^{n-1}\right] \\
&-\left[\frac{\mu\,(w' + w - 1)}{2\triangle x} + \frac{\triangle x}{4\triangle t} - \frac{\nu a}{4}\right]\left[v_{j+1}^n - v_j^n - v_{j+1}^{n-1} + v_j^{n-1}\right] \\
&+\frac{\nu\mu}{4\triangle x^2}\left[\left(u_{j+2}^{n-1} - 2u_{j+1}^{n-1} + u_j^{n-1}\right) - \left(u_{j+1}^{n-1} - 2u_j^{n-1} + u_{j-1}^{n-1}\right) - \right. \\
&\left.\left(u_{j+2}^n - 2u_{j+1}^n + u_j^n\right) + \left(u_{j+1}^n - 2u_j^n + u_{j-1}^n\right)\right]
\end{aligned} \tag{6.15}$$

$$\begin{aligned}
&[FDE4(u,v)]_{j+\frac{1}{2}}^{n-\frac{1}{2}} \stackrel{def}{=} \\
&\frac{1}{4}\left[v_{j+1}^n + v_j^n + v_{j+1}^{n-1} + v_j^{n-1}\right] \\
&+\frac{\nu\xi}{4\,(1-\nu^2)\triangle x}\left[\left(u_{j+2}^{n-1} - 2u_{j+1}^{n-1} + u_j^{n-1}\right) + \left(u_{j+1}^{n-1} - 2u_j^{n-1} + u_{j-1}^{n-1}\right) + \right. \\
&\left.\left(u_{j+2}^n - 2u_{j+1}^n + u_j^n\right) + \left(u_{j+1}^n - 2u_j^n + u_{j-1}^n\right)\right] \\
&-\frac{1}{2\,(1-\nu^2)\triangle x}\left[u_{j+1}^n - u_j^n + u_{j+1}^{n-1} - u_j^{n-1}\right] \\
&-\frac{\nu}{2\,(1-\nu^2)\triangle x}\left[u_{j+1}^n - u_{j+1}^{n-1} + u_j^n - u_j^{n-1}\right] \\
&-\frac{\xi\,(w - w')}{2\,(1-\nu^2)}\left[v_{j+1}^n - v_{j+1}^{n-1} + v_j^n - v_j^{n-1}\right]
\end{aligned} \tag{6.16}$$

As before, let $\tilde{u}(x,t)$ and $\tilde{v}(x,t)$ be smooth functions, and let $\tilde{p}$ be defined by Eq. (6.6). Then the errors $ER3$ and $ER4$ in the approximation of $[PDE1(\tilde{u})]_{j+\frac{1}{2}}^{n-\frac{1}{2}}$ and $[PDE2(\tilde{p})]_{j+\frac{1}{2}}^{n-\frac{1}{2}}$ by $[FDE3(\tilde{u},\tilde{v})]_{j+\frac{1}{2}}^{n-\frac{1}{2}}$ and $[FDE4(\tilde{u},\tilde{v})]_{j+\frac{1}{2}}^{n-\frac{1}{2}}$ are defined by

$$[ER3]_{j+\frac{1}{2}}^{n-\frac{1}{2}} \stackrel{def}{=} [FDE3(\tilde{u},\tilde{v})]_{j+\frac{1}{2}}^{n-\frac{1}{2}} - [PDE1(\tilde{u})]_{j+\frac{1}{2}}^{n-\frac{1}{2}} \tag{6.17}$$

$$[ER4]_{j+\frac{1}{2}}^{n-\frac{1}{2}} \stackrel{def}{=} [FDE4(\tilde{u},\tilde{v})]_{j+\frac{1}{2}}^{n-\frac{1}{2}} - [PDE2(\tilde{p})]_{j+\frac{1}{2}}^{n-\frac{1}{2}} \tag{6.18}$$

With the aid of Taylor expansions, it may be shown that

$$\begin{aligned}
[ER3]_{j+\frac{1}{2}}^{n-\frac{1}{2}} &= -\mu\frac{\partial\tilde{p}}{\partial x} - \mu\left(w'+w-1\right)\frac{\partial^2\tilde{v}}{\partial x\,\partial t}\triangle t + \frac{\partial^3\tilde{u}}{\partial x^2\partial t}\frac{\triangle x^2}{8} + \frac{\partial^3\tilde{u}}{\partial t^3}\frac{\triangle t^2}{24} \\
&\quad + a\frac{\partial^3\tilde{u}}{\partial x^3}\frac{\triangle x^2}{24} + a\frac{\partial^3\tilde{u}}{\partial x\,\partial t^2}\frac{\triangle t^2}{8} - \mu\frac{\partial^3\tilde{v}}{\partial x^3}\frac{\triangle x^2}{24} - \mu\frac{\partial^3\tilde{v}}{\partial x\,\partial t^2}\frac{\triangle t^2}{8} \\
&\quad + \frac{1}{8}\frac{\partial^2\tilde{v}}{\partial x\,\partial t}\left[a^2\triangle t^2 - \triangle x^2\right] - a\mu\frac{\partial^4\tilde{u}}{\partial x^3\partial t}\frac{\triangle t^2}{4} + O\left(\triangle^3\right)
\end{aligned} \tag{6.19}$$

It may similarly be shown that

$$\begin{aligned}
&[ER4]_{j+\frac{1}{2}}^{n-\frac{1}{2}} \\
&= \frac{-\nu\,\triangle t}{(1-\nu^2)\,\triangle x}\left[\frac{\partial\tilde{u}}{\partial t} + a\frac{\partial\tilde{u}}{\partial x} - \mu\frac{\partial^2\tilde{u}}{\partial x^2}\right] - \frac{\xi\,(w-w')}{(1-\nu^2)}\frac{\partial\tilde{v}}{\partial t}\triangle t \\
&\quad - \frac{\xi\,(w-w')}{(1-\nu^2)}O\left(\triangle^3\right) + \frac{\partial^2\tilde{v}}{\partial x^2}\frac{\triangle x^2}{8} + \frac{\partial^2\tilde{v}}{\partial t^2}\frac{\triangle t^2}{8} \\
&\quad + \frac{\nu\xi\,\triangle x}{24\,(1-\nu^2)}\left[5\frac{\partial^4\tilde{u}}{\partial x^4}\triangle x^2 + 3\frac{\partial^4\tilde{u}}{\partial x^2\partial t^2}\triangle t^2\right] \\
&\quad - \frac{1}{24\,(1-\nu^2)}\left[\frac{\partial^3\tilde{u}}{\partial x^3}\triangle x^2 + 3\frac{\partial^3\tilde{u}}{\partial x\,\partial t^2}\triangle t^2\right] \\
&\quad - \frac{\nu\,\triangle t}{24\,(1-\nu^2)\,\triangle x}\left[3\frac{\partial^3\tilde{u}}{\partial x^2\partial t}\triangle x^2 + \frac{\partial^3\tilde{u}}{\partial t^3}\triangle t^2\right] + O\left(\triangle^3\right) \\
&\quad + \frac{\nu\xi\,\triangle x}{(1-\nu^2)}O\left(\triangle^3\right) - \frac{1}{(1-\nu^2)}O\left(\triangle^3\right) - \frac{\nu\,\triangle t}{(1-\nu^2)\,\triangle x}O\left(\triangle^3\right)
\end{aligned} \tag{6.20}$$

In Eqs. (6.19) and (6.20), all derivatives are evaluated at $((j+1/2)\,\triangle x, (n-1/2)\,\triangle t)$.

It is seen that the expressions for $ER3$ and $ER4$ are very similar to those for $ER1$ and $ER2$. The same remarks made regarding the consistency and truncation error of the a-$\mu(I1)$ scheme are applicable to the a-$\mu(I2)$ scheme.

The main conclusion of this section is that if (i) $\nu^2 \neq 1$, (ii) the rule of mesh refinement is such that $\frac{\triangle t}{\triangle x}$ remains bounded as $\triangle x \to 0$ and $\triangle t \to 0$, and (iii) $w = w' = 1/2$, then the interior discrete equations of the a-$\mu(I1)$ and a-$\mu(I2)$ schemes are consistent with the advection-diffusion equation $PDE1(\tilde{u}) = 0$ and with $PDE2(\tilde{p}) = 0$, and the schemes are second-order accurate in space and time.

7 Filtering of the Initial Conditions

The accuracy of the solution may be improved by a modification of given initial conditions. This modification represents a filtering out of spurious components from the numerical representation of given initial conditions.

Let $\Delta t = 0$, i.e., $\nu = \xi = 0$. Then Eqs. (4.9) and (4.10) of the a-$\mu(I1)$ scheme become, for $j = 1, \ldots, J-1$,

$$\left(u_x^+\right)_j^n = \frac{1}{2}\left[u_{j+1}^{n-1} - \left(u_x^+\right)_{j+1}^{n-1} - u_{j-1}^{n-1} - \left(u_x^+\right)_{j-1}^{n-1}\right] \tag{7.1}$$

and

$$u_j^n = \frac{1}{2}\left[u_{j+1}^{n-1} - \left(u_x^+\right)_{j+1}^{n-1} + u_{j-1}^{n-1} + \left(u_x^+\right)_{j-1}^{n-1}\right] \tag{7.2}$$

Eqs. (7.1) and (7.2) can be rewritten as

$$\begin{aligned} &\frac{1}{2}\left[\left(u_x^+\right)_j^n + \left(u_x^+\right)_j^{n-1}\right] \\ = \;& \frac{1}{4}\left[u_{j+1}^{n-1} - u_{j-1}^{n-1} + 2\left(u_x^+\right)_j^{n-1} - \left(u_x^+\right)_{j+1}^{n-1} - \left(u_x^+\right)_{j-1}^{n-1}\right] \end{aligned} \tag{7.3}$$

and

$$\begin{aligned} &\frac{1}{2}\left[u_j^n + u_j^{n-1}\right] \\ = \;& \frac{1}{4}\left[u_{j+1}^{n-1} + u_{j-1}^{n-1} + 2u_j^{n-1} - \left(u_x^+\right)_{j+1}^{n-1} + \left(u_x^+\right)_{j-1}^{n-1}\right] \end{aligned} \tag{7.4}$$

where the terms on the right hand sides of Eqs. (7.1)–(7.4) are all known from the initial time level, given by Eqs. (3.17) and (3.18).

Corresponding to Eqs. (7.3) and (7.4), the conservation equations (3.15) and (3.16) at the boundaries can be written as

$$\frac{1}{2}\left[\left(u_x^+\right)_j^n + \left(u_x^+\right)_j^{n-1}\right] = \frac{1}{2}\left[u_{j+1}^{n-1} - u_j^n + \left(u_x^+\right)_j^{n-1} - \left(u_x^+\right)_{j+1}^{n-1}\right] \quad , \quad j = 0 \tag{7.5}$$

and

$$\frac{1}{2}\left[\left(u_x^+\right)_j^n + \left(u_x^+\right)_j^{n-1}\right] = \frac{1}{2}\left[u_j^n - u_{j-1}^{n-1} + \left(u_x^+\right)_j^{n-1} - \left(u_x^+\right)_{j-1}^{n-1}\right] \quad , \quad j = J \tag{7.6}$$

where the right hand sides of Eqs. (7.5) and (7.6) are known from the initial time level or the boundary values.

Eqs. (7.1), (7.2), (3.19), (3.20), (7.5) and (7.6) serve to determine 'filtered' initial values. The von Neumann stability analysis of the interior filtering 'scheme' is performed as previously, with the substitution of Eq. (5.1) to obtain the form of Eq. (5.2) where

$$Q^{(1)} = \begin{bmatrix} 1 & 1 \\ 1 & -1 \end{bmatrix} \qquad \text{and} \qquad Q^{(2)} = \begin{bmatrix} e^{i\theta} & -e^{i\theta} \\ e^{-i\theta} & e^{-i\theta} \end{bmatrix} \tag{7.7}$$

Thus $\left[Q^{(1)}\right]^{-1} = \frac{1}{2}Q^{(1)}$ and therefore the amplification matrix of the interior filtering scheme is given by

$$G = \left[Q^{(1)}\right]^{-1} Q^{(2)} = \begin{bmatrix} \cos\theta & -i\sin\theta \\ i\sin\theta & -\cos\theta \end{bmatrix} \tag{7.8}$$

8 The Dual-Mesh Explicit a-μ Scheme

In this section, we present an explicit numerical scheme to solve Eq. (1.2). It differs from the explicit a-μ scheme presented in [1, 6] in that the diffusion term in Eq. (1.2) is better modeled in the current explicit scheme, and the diffusion flux in Eq. (3.6) is modeled more flexibly. These differences both introduce a coupling between the meshes Ω_1 and Ω_2. This is in contrast to the explicit a-μ scheme of [1, 6], which is formulated on Ω_1 (or Ω_2) exclusively. Hence, the present explicit scheme will be termed the dual-mesh explicit a-μ scheme.

The explicit scheme will be presented by indicating the modifications to the a-$\mu(I1)$ scheme to change it to an explicit scheme. The dual space-time mesh, the SEs, and the CEs are defined as for the a-$\mu(I1)$ scheme. The numerical representation defined in Eq. (2.1) is also assumed. We continue to take advantage of the notation defined in Eqs. (3.10) and (3.11). Instead of using Eq. (3.4), the diffusion term in that equation will be lagged. Thus, instead of using Eq. (3.12), the unknown $\left(u_t^+\right)_j^n$ at the time step n will be expressed as

$$\left(u_t^+\right)_j^n = -\nu\left(u_x^+\right)_j^n + \frac{\xi}{4}\left[\left(u_x^+\right)_{j+1}^{n-1} - \left(u_x^+\right)_{j-1}^{n-1}\right] \quad , \qquad 0 < j < J. \tag{8.1}$$

However, the known quantity $\left(u_t^+\right)_j^{n-1}$ at the time level $n-1$ continues to be calculated from Eq. (3.12), rather than from Eq. (8.1). Calculation of $\left(u_t^+\right)_j^{n-1}$ from Eq. (8.1) would result in a three-time-level scheme, which would require additional computer memory and would require knowledge of the solution at $n = 1$ in addition to the initial condition at $n = 0$.

The definition of the diffusion flux is also altered by setting $w' = 0$ in Eq. (3.7), so that for $(x,t) \in \mathrm{SE}(j,n)$,

$$u_x^*(x,t\,;j,n) \stackrel{\text{def}}{=} \begin{cases} w(u_x)_j^n + \overline{w}(u_x)_j^{n-1} \,, & \text{if } t \le t^n; \\ (u_x)_j^n \,, & \text{if } t > t^n. \end{cases} \tag{8.2}$$

where w is a weighting factor to be specified, and $\overline{w} \stackrel{def}{=} 1 - w$. This definition is used to complete the definition of the numerical space-time flux in Eq. (3.6). The numerical flux analogue is required to satisfy conservation over the CEs. Thus, Eqs. (2.6) are required to be satisfied. With the modifications described above, this leads to Eqs. (3.13) and (3.14) being replaced by

$$\left[u_j^n + \left(u_x^+\right)_j^n\right] - \left[u_{j+1}^{n-1} - \left(u_x^+\right)_{j+1}^{n-1}\right]$$

$$
\begin{aligned}
&-\nu\left[u_j^n-\left(u_t^+\right)_j^n\right]+\xi\left[w(u_x^+)_j^n+\overline{w}(u_x^+)_j^{n-1}\right]\\
&+\nu\left[u_{j+1}^{n-1}+\left(u_t^+\right)_{j+1}^{n-1}\right]-\xi(u_x^+)_{j+1}^{n-1}\\
=\;& 0\quad,\qquad 0\le j<J
\end{aligned}
\tag{8.3}
$$

and

$$
\begin{aligned}
&\left[u_j^n-\left(u_x^+\right)_j^n\right]-\left[u_{j-1}^{n-1}+\left(u_x^+\right)_{j-1}^{n-1}\right]\\
&+\nu\left[u_j^n-\left(u_t^+\right)_j^n\right]-\xi\left[w(u_x^+)_j^n+\overline{w}(u_x^+)_j^{n-1}\right]\\
&-\nu\left[u_{j-1}^{n-1}+\left(u_t^+\right)_{j-1}^{n-1}\right]+\xi(u_x^+)_{j-1}^{n-1}\\
=\;& 0\quad,\qquad 0<j\le J.
\end{aligned}
\tag{8.4}
$$

As with the implicit schemes, the discretized initial and boundary information required by the scheme will be assumed to be given by Eqs. (3.17)–(3.22). However, the same remarks as before apply more general treatment of the initial and boundary conditions. Collecting terms in Eqs. (8.3) and (8.4), we obtain

$$
\begin{aligned}
&(1-\nu)\,u_j^n+(1+w\xi)\left(u_x^+\right)_j^n+\nu\left(u_t^+\right)_j^n\\
=\;&(1-\nu)\,u_{j+1}^{n-1}-(1-\xi)\left(u_x^+\right)_{j+1}^{n-1}-\overline{w}\xi\left(u_x^+\right)_j^{n-1}-\nu\left(u_t^+\right)_{j+1}^{n-1}
\end{aligned}
\tag{8.5}
$$

and

$$
\begin{aligned}
&(1+\nu)\,u_j^n-(1+w\xi)\left(u_x^+\right)_j^n-\nu\left(u_t^+\right)_j^n\\
=\;&(1+\nu)\,u_{j-1}^{n-1}+(1-\xi)\left(u_x^+\right)_{j-1}^{n-1}+\overline{w}\xi\left(u_x^+\right)_j^{n-1}+\nu\left(u_t^+\right)_{j-1}^{n-1}\;.
\end{aligned}
\tag{8.6}
$$

Eq. (8.5) is valid for $0\le j<J$. Together with the boundary condition Eq. (3.19), it supplies one equation per mesh point (j,n), $0\le j\le J$. Eq. (8.6) is valid for $0<j\le J$ at the time level n. Together with the boundary condition Eq. (3.20), it also supplies one equation per mesh point (j,n), $0\le j\le J$. The quantities $\left(u_t^+\right)_{j-1}^{n-1}$ and $\left(u_t^+\right)_{j+1}^{n-1}$ appearing in Eqs. (8.5) and (8.6) are known from the previous time level $n-1$, through Eq. (3.12), or from the boundary data Eqs. (3.21) and (3.22). The quantities $\left(u_t^+\right)_j^n$ at the current time-level n will be eliminated from Eqs. (8.5) and (8.6) as follows.

For $j=0$, the known boundary data from Eqs. (3.19) and (3.21) are used in Eq. (8.5) to yield

$$
(1+w\xi)\left(u_x^+\right)_j^n=(S_+)_j^{n-1}\,,\qquad j=0,
\tag{8.7}
$$

where

$$
\begin{aligned}
(S_+)_j^{n-1}\;=\;&(1-\nu)\,u_{j+1}^{n-1}-(1-\xi)\left(u_x^+\right)_{j+1}^{n-1}-\overline{w}\xi\left(u_x^+\right)_j^{n-1}-\nu\left(u_t^+\right)_{j+1}^{n-1}\\
&-(1-\nu)\,u_j^n-\nu\left(u_t^+\right)_j^n
\end{aligned}
$$

Eq. (8.7) and the boundary condition Eq. (3.19) constitute two equations at $j = 0$.

For $1 \leq j \leq J-1$, we substitute for $\left(u_t^+\right)_j^n$ from Eq. (8.1) in Eq. (8.5) to obtain

$$(1-\nu)\, u_j^n + \left(1 - \nu^2 + w\xi\right) \left(u_x^+\right)_j^n = (S_+)_j^{n-1} \tag{8.8}$$

where

$$\begin{aligned}(S_+)_j^{n-1} &= (1-\nu)\, u_{j+1}^{n-1} - \left(1 - \xi + \frac{\nu\xi}{4}\right) \left(u_x^+\right)_{j+1}^{n-1} - \overline{w}\xi \left(u_x^+\right)_j^{n-1} \\ &\quad + \frac{\nu\xi}{4} \left(u_x^+\right)_{j-1}^{n-1} - \nu \left(u_t^+\right)_{j+1}^{n-1}\end{aligned}$$

Similarly, for $1 \leq j \leq J-1$, we substitute for $\left(u_t^+\right)_j^n$ from Eq. (8.1) in Eq. (8.5) to obtain

$$(1+\nu)\, u_j^n - \left(1 - \nu^2 + w\xi\right) \left(u_x^+\right)_j^n = (S_-)_j^{n-1} \tag{8.9}$$

where

$$\begin{aligned}(S_-)_j^{n-1} &= (1+\nu)\, u_{j-1}^{n-1} + \left(1 - \xi - \frac{\nu\xi}{4}\right) \left(u_x^+\right)_{j-1}^{n-1} + \overline{w}\xi \left(u_x^+\right)_j^{n-1} \\ &\quad + \frac{\nu\xi}{4} \left(u_x^+\right)_{j+1}^{n-1} + \nu \left(u_t^+\right)_{j-1}^{n-1} .\end{aligned}$$

Eqs. (8.8) and (8.9) constitute two equations at each mesh point (j, n) such that $1 \leq j \leq J-1$.

Finally, at $j = J$, the known boundary data from Eqs. (3.20) and (3.22) are used in Eq. (8.6) to yield

$$-(1 + w\xi) \left(u_x^+\right)_j^n = (S_-)_j^{n-1}, \qquad j = J, \tag{8.10}$$

where

$$\begin{aligned}(S_-)_j^{n-1} &= (1+\nu)\, u_{j-1}^{n-1} + (1-\xi) \left(u_x^+\right)_{j-1}^{n-1} + \overline{w}\xi \left(u_x^+\right)_j^{n-1} + \nu \left(u_t^+\right)_{j-1}^{n-1} \\ &\quad - (1+\nu)\, u_j^n + \nu \left(u_t^+\right)_j^n\end{aligned}$$

Eq. (8.10) and the boundary condition Eq. (3.20) constitute two equations at a boundary mesh point with $j = J$.

All mesh variables on the right-hand sides of Eqs. (8.7), (8.8), (8.9) and (8.10) are known from the marching variables at the previous time level or from boundary values. The system of equations described above, with two equations per mesh point, enable a marching step in which the solution u_j^n and $(u_x^+)_j^n$ at the current time level n can be determined by explicit solution. The explicit solution process will now be discussed. At the left boundary $j = 0$, u_j^n is known from the boundary condition, Eq. (3.19), while $(u_x^+)_j^n$ is obtained from Eq. (8.7) as

$$\left(u_x^+\right)_j^n = (S_+)_j^{n-1} \;/\; (1 + w\xi) \tag{8.11}$$

At the right boundary $j = J$, u_j^n is known from the boundary condition, Eq. (3.20), while $(u_x^+)_j^n$ is obtained from Eq. (8.10) as

$$\left(u_x^+\right)_j^n = -\left(S_-\right)_j^{n-1} / \left(1 + w\xi\right) \tag{8.12}$$

At a mesh point (j, n) with $1 \leq j \leq J-1$, u_j^n and $(u_x^+)_j^n$ are obtained by solving Eqs. (8.8) and (8.9) simultaneously to yield

$$u_j^n = \frac{1}{2}\left[\left(S_+\right)_j^{n-1} + \left(S_-\right)_j^{n-1}\right] \tag{8.13}$$

and

$$\left(u_x^+\right)_j^n = \frac{1}{2\left(1 - \nu^2 + w\xi\right)}\left[\left(1+\nu\right)\left(S_+\right)_j^{n-1} - \left(1-\nu\right)\left(S_-\right)_j^{n-1}\right] . \tag{8.14}$$

Thus the solution at the new time level can be explicitly calculated. Note that Eq. (8.13), which does not involve $(u_x^+)_j^n$, is obtained by simply adding together the conservation equations (8.8) and (8.9). It represents flux conservation for $\mathrm{CE}(j,n)$, the union of $\mathrm{CE}_+(j,n)$ and $\mathrm{CE}_-(j,n)$.

The following important facts should be noted. The boundary information is used in the dual-mesh explicit scheme in the same way as it is used in the a-$\mu(I1)$ scheme, i.e., the boundary equations of the two schemes are the same. If the conditions

$$u_j^n = u_j^{n-1} \qquad ; \qquad \left(u_x^+\right)_j^n = \left(u_x^+\right)_j^{n-1} \tag{8.15}$$

hold for $0 \leq j \leq J$ and some $n = N$, then the remaining equations of the dual-mesh explicit a-μ scheme written at the time level N become identical with those of the a-$\mu(I1)$ scheme written at the same time level. Specifically, Eqs. (8.1) and (3.12) become identical, Eqs. (8.2) and (3.7) become identical, and therefore the integral conservation relations Eqs. (8.5) and (8.6) of the dual-mesh explicit scheme become identical with those of the a-$\mu(I1)$ scheme, Eqs. (3.15) and (3.16), respectively. Hence, solution time-slices u_j^n and u_j^{n-1} that satisfy the condition (8.15) and the discretized equations of the dual-mesh explicit scheme, will also satisfy the discretized equations of the a-$\mu(I1)$ scheme.

Next, the stability of the dual-mesh explicit scheme will be discussed. For $1 < j < J-1$, we substitute for $\left(u_t^+\right)_j^n$ from Eq. (8.1) and for $\left(u_t^+\right)_{j-1}^{n-1}$ and $\left(u_t^+\right)_{j+1}^{n-1}$ from Eq. (3.12) in Eqs. (8.5) and (8.6) to obtain the interior equations of the scheme in terms of u_j^n and $(u_x^+)_j^n$, i.e.,

$$\begin{aligned} & \left(1-\nu\right)u_j^n + \left(1 - \nu^2 + w\xi\right)\left(u_x^+\right)_j^n \\ = \; & \left(1-\nu\right)u_{j+1}^{n-1} - \frac{\nu\xi}{4}\left(u_x^+\right)_{j+2}^{n-1} - \left[1 - \nu^2 - \xi\left(1 - \frac{\nu}{4}\right)\right]\left(u_x^+\right)_{j+1}^{n-1} \\ & + \left(\frac{\nu}{4} - \overline{w}\right)\xi\left(u_x^+\right)_j^{n-1} + \frac{\nu\xi}{4}\left(u_x^+\right)_{j-1}^{n-1} \end{aligned} \tag{8.16}$$

and

$$
\begin{aligned}
& (1+\nu)\, u_j^n - \left(1-\nu^2+w\xi\right)\left(u_x^+\right)_j^n \\
= \; & (1+\nu)\, u_{j-1}^{n-1} - \frac{\nu\xi}{4}\left(u_x^+\right)_{j-2}^{n-1} + \left[1-\nu^2-\xi\left(1+\frac{\nu}{4}\right)\right]\left(u_x^+\right)_{j-1}^{n-1} \\
& + \left(\frac{\nu}{4}+\overline{w}\right)\xi\left(u_x^+\right)_j^{n-1} + \frac{\nu\xi}{4}\left(u_x^+\right)_{j+1}^{n-1}
\end{aligned} \tag{8.17}
$$

Let $1-\nu^2+w\xi \neq 0$. Then, as is shown by Eqs. (8.13) and (8.14), the interior equations (8.16) and (8.17) can be solved for u_j^n and $(u_x^+)_j^n$. Let $\overrightarrow{q}(j,n)$ be given defined by Eq. (3.33). Then this solution is written in the form

$$
\begin{aligned}
& \overrightarrow{q}(j,n) \\
= \; & Q_{-2}\,\overrightarrow{q}(j-2,n-1) + Q_{-2}\,\overrightarrow{q}(j-2,n-1) + Q_0\,\overrightarrow{q}(j,n-1) \\
& Q_1\,\overrightarrow{q}(j+1,n-1) + Q_2\,\overrightarrow{q}(j+2,n-1)
\end{aligned}
$$

i.e.

$$
\overrightarrow{q}(j,n) = \sum_{l=-2}^{2} Q_l\,\overrightarrow{q}(j+l,n-1) \tag{8.18}
$$

where

$$
Q_{-2} \stackrel{def}{=} \frac{1}{2}\begin{pmatrix} 0 & -\frac{\nu\xi}{4} \\ 0 & \frac{\nu\xi(1-\nu)}{4(1-\nu^2+w\xi)} \end{pmatrix} \tag{8.19}
$$

$$
Q_{-1} \stackrel{def}{=} \frac{1}{2}\begin{pmatrix} 1+\nu & 1-\nu^2-\xi \\ -\left(\frac{1-\nu^2}{1-\nu^2+w\xi}\right) & \frac{\xi\left(1-\frac{\nu}{2}\right)-(1-\nu)\left(1-\nu^2\right)}{1-\nu^2+w\xi} \end{pmatrix} \tag{8.20}
$$

$$
Q_0 \stackrel{def}{=} \frac{1}{2}\begin{pmatrix} 0 & \frac{\nu\xi}{2} \\ 0 & \frac{2\xi\left(w-1+\frac{\nu^2}{4}\right)}{1-\nu^2+w\xi} \end{pmatrix} \tag{8.21}
$$

$$
Q_1 \stackrel{def}{=} \frac{1}{2}\begin{pmatrix} 1-\nu & -\left(1-\nu^2-\xi\right) \\ \frac{1-\nu^2}{1-\nu^2+w\xi} & \frac{\xi\left(1+\frac{\nu}{2}\right)-(1+\nu)\left(1-\nu^2\right)}{1-\nu^2+w\xi} \end{pmatrix} \tag{8.22}
$$

$$
Q_2 \stackrel{def}{=} \frac{1}{2}\begin{pmatrix} 0 & -\frac{\nu\xi}{4} \\ 0 & \frac{-\nu\xi(1+\nu)}{4(1-\nu^2+w\xi)} \end{pmatrix} \tag{8.23}
$$

The stability analysis procedure is the same as that used in Section 5 for the implicit schemes. When the substitution of Eq. (5.1) is made in Eq. (8.18), the result is

$$
\vec{q}^*(n,\theta) = Q(\nu,\xi,w,\theta)\;\vec{q}^*(n-1,\theta)\;. \tag{8.24}
$$

Here,

$$
Q(\nu,\xi,w,\theta) = \sum_{l=-2}^{2} e^{il\theta}Q_l = \begin{bmatrix} Q_{11} & Q_{12} \\ Q_{21} & Q_{22} \end{bmatrix} \tag{8.25}
$$

where

$$Q_{11} = \cos\theta - i\nu\sin\theta \tag{8.26}$$

$$Q_{12} = \frac{1}{2}\left[\nu\xi\sin^2\theta - 2i\left(1-\nu^2-\xi\right)\sin\theta\right] \tag{8.27}$$

$$Q_{21} = i\left(1-\nu^2\right)\sin\theta \,/\, \left(1-\nu^2+w\xi\right) \tag{8.28}$$

$$\begin{aligned} Q_{22} = \frac{1}{2\left(1-\nu^2+w\xi\right)}\Bigg\{&\frac{-\nu\xi}{2}\left(\nu\cos 2\theta + i\sin 2\theta\right) + 2\xi\left(w-1+\frac{\nu^2}{4}\right) \\ &-2\left(1-\nu^2-\xi\right)\cos\theta + i\left[\nu\xi - 2\nu\left(1-\nu^2\right)\right]\sin\theta\Bigg\} \end{aligned} \tag{8.29}$$

Examination of Eq. (8.24) shows that $Q(\nu,\xi,w,\theta)$ is the amplification matrix for the interior scheme. The eigenvalues of Q are the amplification factors. An eigenvalue λ of Q satisfies Eq. (5.10) with

$$A = 2\left(1-\nu^2+w\xi\right) \tag{8.30}$$

$$\begin{aligned} B = &-\xi\left[2(1+w)\cos\theta + \nu^2\sin^2\theta + 2(w-1)\right] \\ &-i\nu\sin\theta\left[(1-2w)\xi - 4\left(1-\nu^2\right) - \xi\cos\theta\right] \end{aligned} \tag{8.31}$$

$$\begin{aligned} C = &\ 2(w-1)\xi\cos\theta - \xi\nu^2\sin^2\theta - 2\left(1-\nu^2+w\xi\right) \\ &+i\nu\xi\sin\theta(1-2w-\cos\theta) \end{aligned} \tag{8.32}$$

The eigenvalues $\lambda_\pm$ have been evaluated numerically for a range of values of ν, ξ, w and θ. These numerical experiments show that if

$$w \geq 2 \tag{8.33}$$

then the dual-mesh explicit scheme is stable provided only that Eq. (5.15) holds, i.e., if $\nu^2 < 1$ and $\xi \geq 0$.

We note the unusual fact that if Eq. (8.33) is satisfied, the magnitude of the viscosity has no influence on the stability condition of the dual-mesh explicit scheme. A similar statement can be made about the explicit a-μ scheme of [6]. This is in contrast to most explicit schemes for diffusion equations, for which the value of ξ is limited by stability constraints. This fact, together with the remarks made earlier concerning the condition (8.15), points to an important possibility for the dual-mesh explicit scheme. The dual-mesh explicit scheme can be used to obtain 'steady-state' time-asymptotic limits of solutions to the convection-diffusion equation in an efficient manner. Time steps as large as those used with the a-$\mu(I1)$ scheme, and limited only by the CFL criterion, can be used. At each time level, fewer airthmetic operations are required for the explicit scheme than for the a-$\mu(I1)$ scheme. This computational advantage would be even greater when multidimensional extensions of the algorithms are considered. The steady-state solution time-slice will be the same as that obtained with the a-$\mu(I1)$ scheme, and thus be second-order accurate in space.

9 Numerical Results

Three test problems will be used to evaluate the accuracy of the implicit a-μ schemes. The weighting factors for the viscous fluxes are taken to be $w = w' = 0.5$ for all the computations run with the implicit schemes. Unless stated otherwise, the a-$\mu(I1)$ scheme was used for the computations in subsections 9.1 through 9.3.

9.1 Decaying Traveling Sine Wave

In the first problem, we consider a special case of Eq. (1.2) ($a = 1$ and $\mu = 0.01$) with $0 \le x \le 1$ and $t \ge 0$. The initial and boundary condition functions $u_I(x)$, $u_L(t)$ and $u_R(t)$ are defined such that they are consistent with a special solution to Eq. (1.2), i.e.,

$$u = u_e(x,t) \stackrel{\text{def}}{=} \exp(-4\pi^2\mu t)\sin\left[2\pi(x-at)\right] \tag{9.1}$$

At any time $t = t^n$, let

$$L_1(u) \stackrel{\text{def}}{=} \frac{1}{(J-1)\exp(-4\pi^2\mu t^n)} \sum_{j=1}^{J-1} |u_j^n - u_e(x_j, t^n)| \tag{9.2}$$

$L_1(u)$ is an error norm (per mesh point) which is normalized by the decay factor of $u_e(x,t)$.

Let $J = 80$ (i.e., $\Delta x = 1/80$) and $\nu = 0.8$ (i.e., $\Delta t = 0.01$). Then $L_1(u) = 0.1641 \times 10^{-3}$ at $t = 4$ (i.e., $n = 400$). Through numerical experiments, it has been shown that $L_1(u)$ at a given time t is reduced by a factor of 4 if both Δx and Δt are reduced by half, confirming the second-order accurate nature of the scheme.

Fig. 8 shows a comparison of the computed solution at $t = 4$ with the exact solution. It also shows the error $u_e(x_j, t^n) - u_j^n$ scaled by the peak magnitude of the exact solution at that time level. It is seen that the maximum error is less than 0.3% of the peak magnitude. The peak magnitude is seen to be just over 0.2.

Fig. 9 shows a comparison of the errors in the solutions obtained with the a-$\mu(I1)$ scheme and the implicit MacCormack scheme ([28]). Both schemes were applied with the same parameters and mesh as described above. It is seen that the current scheme is considerably more accurate than the implicit MacCormack scheme. Refinement of the grid keeping v constant would actually make the comparison even more favorable. This is because the implicit MacCormack scheme is second-order accurate in space and time only if ξ is held constant and $\nu \to 0$ when refining the grid.

9.2 Pure Diffusion

We consider a special case of the convection-diffusion equation with $a = 0$ and $\mu = 1$, in the domain $0 \le x \le 1$ and $t \ge 0$. The initial/boundary conditions completing the problem specification are (i) $u(0,t) = u(1,t) = 0$ for $t \ge 0$, (ii) $u(x,0) = 2x$ for $0 \le x \le 0.5$, and (iii) $u(x,0) = 2(1-x)$ for $0.5 \le x \le 1$. The solution $u(x,t)$ exhibits the diffusive decay of the initial sawtooth shape. An exact series solution is available, see for e.g. p.15 of [29]. For the CE/SE computation, uniform mesh intervals $\Delta x = 0.02$ and $\Delta t = 0.005$ are used.

Fig. 10 shows the time-slice at $t = 0.05$, comparing numerical and exact solutions, and also showing the error scaled with the peak exact value at that time level. The maximum error magnitude is seen to be about 0.5% of the peak solution value. At $t = 1$ (not shown), when the peak solution value has dwindled to about 4×10^{-5}, the maximum error magnitude is about 0.15% of the peak solution value.

The same problem on the same mesh was solved with the Crank-Nicolson scheme, which is probably the best traditional scheme for the parabolic pure diffusion equation. Fig. 11 shows a comparison between the current scheme and the Crank-Nicolson scheme, at $t = 0.05$. The schemes are seen to be of similar accuracy, as is to be expected from the identity of the amplification factors. The current scheme is seen to be slightly more accurate for this case.

9.3 Steady State Boundary Layer

We next consider the problem defined for the convection-diffusion equation in the domain $0 \leq x \leq 1$ and $t \geq 0$ by the conditions (i) $u(0,t) = 0$ for $t \geq 0$, (ii) $u(1,t) = 1$ for $t \geq 0$, and (iii) $u(x,0) = x$ for $0 \leq x \leq 1$. The 'steady-state' or time-asymptotic limit of the solution is $u(x,\infty) = [\exp(ax/\mu) - 1] \,/\, [\exp(a/\mu) - 1]$.

The case $a = 1$, $\mu = 1$ (i.e., 'Reynolds' number $\mathrm{Re} = a/\mu = 1$) is first considered. Fig. 12 shows the steady-state limit of the numerical solution, compared with the exact steady-state limit. With only three interior mesh points, the numerical solution has a maximum error of about 0.001.

In Fig. 13, we compare the errors in the a-$\mu(I1)$ and a-$\mu(I2)$ solutions for the same problem, but with $\mu = 0.1$, so that $\mathrm{Re} = 10$, which leads to a steady-state boundary layer at $x = 1$. Mesh spacing $\Delta x = 0.05$ was used. The two schemes yield very similar results.

The final case considered is the same problem, but with $\mu = 0.01$, so that $\mathrm{Re} = 100$. This leads to the formation of a fairly sharp boundary layer, because the thickness of the layer scales as the inverse of the Reynolds number. Uniform mesh intervals $\Delta x = 0.0025$ and $\Delta t = 0.002$ are used, so that the Courant number is 0.8. Fig. 14 shows the computed and exact steady-state limits, together with the error. The boundary layer is seen to be well resolved, with the maximum magnitude of the error being about 1% of the solution peak.

9.4 Calculations with the Dual-Mesh Explicit Scheme

In this subsection, we examine results obtained with the dual-mesh explicit a-μ scheme for the same problems as in subsections 9.1 and 9.3. The value of the weighting factor w in the dual-mesh explicit scheme was always taken to be 2.

Fig. 15 shows the solution time-slice at $t = 4$, computed with the dual-mesh explicit scheme, for the same problem as considered in subsection 9.1. The same spatial and temporal mesh intervals were used as in subsection 9.1, so that Fig. 15 can be compared with Fig. 8. It is seen that the a-$\mu(I1)$ scheme is considerably more accurate than the dual-mesh explicit scheme, owing to the latter being only first-order accurate in time. The peak error in Fig. 15 is just over 7% of the solution peak, as compared to only about 0.2% in Fig. 8. The result obtained for the same problem with the same mesh parameters, using the explicit a-$\mu(I1)$ scheme of [6] is shown in Fig. 16. The error plotted in Fig. 16 is very similar to that in Fig.

15. This shows that the error is dominated by that arising from the first-order-time-accurate modeling of the viscous fluxes in the integral conservation equations in both explicit schemes. Fig. 17 shows the solution time-slice at $t = 4$, computed with the dual-mesh explicit scheme, but using a time step that is four times smaller than that used for Fig. 15, while keeping the spatial mesh intervals the same. The error is smaller by about a factor of ten than that in Fig. 15. Numerical experiments show that the numerical space-time solution can be made to approach the exact solution as closely as desired by refining the mesh with a refinement rule that holds ξ constant rather than ν, so that Δt is reduced proportionally to Δx^2 rather than to Δx. The same is true of the explicit a-$\mu(I1)$ scheme of [6]. For multidimensional flows, the explicit schemes could have an advantage over the implicit a-$\mu(I1)$ and a-$\mu(I2)$ schemes, with regard to computational cost to achieve a given level of accuracy.

The dual-mesh explicit scheme was also applied to the 'boundary layer' problem of subsection 9.3. Fig. 18 shows the 'steady-state' limiting behavior of the numerical solution, at $t = 3$. The computation was performed with the same values of Δx, Δt, ν, and ξ as were used for the a-$\mu(I1)$ scheme in subsection 9.3. The same initial and boundary conditions were used. From Figs. 14 and 18, and from an examination of the computer printout of the values, the steady-state limit reached by the a-$\mu(I1)$ and dual-mesh explicit schemes are the same. This is to be expected, on the basis of the remarks at the end of Section 8. Fig. 19 shows the 'steady-state' solution time-slice obtained with the explicit a-μ scheme of [6], using the same conditions as for the other schemes. There is seen to be a considerable error in the steady-state limit, owing to the lack of modeling of physical diffusion in the discretized differential form of the conservation law. This error can be reduced to match the error level in Fig. 18, at the cost of increased computation, by reducing Δt and perhaps reducing Δx.

For multiple spatial dimensions, the computational cost of an implicit time-step is generally much higher than that of an explicit time-step. The analysis of the dual-mesh explicit scheme, confirmed by the numerical results, shows that the scheme can be used to obtain the same steady-state limit as with the a-$\mu(I1)$ scheme. It is expected that for most steady-state results, the steady state can be reached in approximately the same number of time steps by the two schemes. Hence, when generalized to multidimensional flows, use of the dual-mesh explicit scheme may be the more efficient way to obtain the steady state with a desired level of accuracy.

10 Summary and Conclusions

In the explicit a-μ scheme [6, 4], the diffusion term in Eq. (1.2) is not modeled, i.e., Eq. (2.3) is assumed. Also the diffusion term in Eq. (1.5) is modeled with no interpolation or extrapolation, with a resulting reduction of time-accuracy. Obviously, such a solver can be used only when the diffusion term is small compared with the convection term. Contrarily, the diffusion terms in both Eqs. (1.2) and (1.5) are modeled in the current implicit solvers. The diffusion term in Eq. (1.2) is also modeled in the present dual-mesh explicit a-μ scheme, although it remains first order accurate in time because of the explicit nature of the modeling

of the diffusion fluxes in Eq. (1.5).

The current implicit and explicit solvers are carefully constructed so that they become identical to the explicit a scheme for the pure convection equation, when the viscosity coefficient vanishes. Because the a scheme is nondissipative, this construction ensures that the physical dissipation is never overwhelmed by numerical dissipation in the present implicit and explicit solvers.

The implicit schemes have been shown to be stable provided the Courant number does not exceed unity in magnitude, for certain ranges of the weighting parameters w and w'. In these cases, there is no dependence of the stability of the schemes on the viscosity parameter. This is true, in particular, for the case $w = w' = 1/2$. Similar remarks concerning the stability are true for the dual-mesh explicit a-μ scheme, for values $w \geq 2$. Stability analysis reveals the remarkable facts that (i) if $\mu = 0$, the amplification factors of the dual-mesh implicit and explicit a-μ schemes reduce to those of the classical Leapfrog scheme, and (ii) if $a = 0$, one of the amplification factors of the implicit a-μ schemes reduces to that of the classical Crank-Nicolson scheme, while one of the amplification factors of the dual-mesh explicit a-μ scheme reduces to that of the DuFort-Frankel scheme.

The truncation error analysis of the discretized equations of the implicit schemes shows that in general they are consistent with the convection-diffusion equation, and are first-order accurate in time. For the case $w = w' = 1/2$, which will be the case used in practice, the scheme is second-order accurate in time and space provided the Courant number remains bounded when refining the space-time mesh. Although a truncation error analysis of the dual-mesh explicit a-μ scheme was not performed, it is evident that the scheme is second-order accurate in space and first-order accurate in time.

Numerical examples have borne out the conclusions of the stability and truncation error analysis. The a-$\mu(I1)$ and a-$\mu(I2)$ schemes have been shown to be similar to each other in their properties and performance. The current implicit schemes were seen from the numerical examples to enable stable accurate computations over the whole viscosity range, from the pure diffusion case to convection dominated problems. The dual-mesh explicit a-μ scheme was shown to be useful for the same range of problems, though needing a smaller time step to achieve comparable accuracy in the time-dependent problems. In the problems where only a steady-state limit is of interest, the dual-mesh explicit a-μ scheme yields the same spatial accuracy as the implicit a-$\mu(I1)$ scheme, with potentially much lower computational cost when extended to problems in multiple spatial dimensions.

The analysis and results noted in this study indicate that the development of the dual-mesh implicit and explicit solvers along similar lines for the time-dependent compressible Navier-Stokes equations may prove equally fruitful.

References

[1] S.C. Chang and W.M. To, "A New Numerical Framework for Solving Conservation Laws – The Method of Space-Time Conservation Element and Solution Element", NASA TM 104495, August 1991.

[2] S.C. Chang, "On an Origin of Numerical Diffusion: Violation of Invariance Under Space-Time Inversion", Proceedings of the 23rd Modeling and Simulation Conference, April 30 - May 1, 1992, Pittsburgh, PA, William G. Vogt and Marlin H. Mickle eds., Part 5, pp. 2727-2738. Also published as NASA TM 105776.

[3] S.C. Chang and W.M. To, "A Brief Description of a New Numerical Framework for Solving Conservation Laws – The Method of Space-Time Conservation Element and Solution Element", Proceedings of the 13th International Conference on Numerical Methods in Fluid Dynamics, July 6-10, 1992, Rome, Italy, M. Napolitano and F. Sabetta, eds. Also published as NASA TM 105757.

[4] S.C. Chang, "New Developments in the Method of Space-Time Conservation Element and Solution Element – Applications to the Euler and Navier-Stokes Equations", Presented at the Second U.S. National Congress on Computational Mechanics, August 16-18, 1993, Washington D.C. Published as NASA TM 106226.

[5] S.C. Chang, X.Y. Wang and C.Y. Chow, "New Developments in the Method of Space-Time Conservation Element and Solution Element – Applications to Two-Dimensional Time-Marching Problems", NASA TM 106758, December 1994.

[6] S.C. Chang, *J. Comput. Phys.*, **119** (1995), pp. 295-324.

[7] S.C. Chang, X.Y. Wang and C.Y. Chow, "The Method of Space-Time Conservation Element and Solution Element – Applications to One-Dimensional and Two-Dimensional Time-Marching Flow Problems", AIAA Paper 95-1754, in A Collection of Technical Papers, 12th AIAA CFD Conference, June 19-22, 1995, San Diego, CA, pp. 1258-1291. Also published as NASA TM 106915.

[8] S.C. Chang, X.Y. Wang, C.Y. Chow and A. Himansu, "The Method of Space-Time Conservation Element and Solution Element – Development of a New Implicit Solver", Proceedings of the Ninth International Conference on Numerical Methods in Laminar and Turbulent Flow, July 10-14, 1995, Atlanta, GA. Also published as NASA TM 106897.

[9] S.C. Chang, C.Y. Loh and S.T. Yu, "Computational Aeroacoustics via a New Global

Conservation Scheme", to appear in the Proceedings of the 15th International Conference on Numerical Methods in Fluid Dynamics, June 24-28, 1996, Monterey, CA.

[10] S.C. Chang, S.T. Yu, A. Himansu, X.Y. Wang and C.Y. Loh, "The Method of Space-Time Conservation Element and Solution Element – A New Paradigm for Numerical Solution of Conservation Laws", to appear in *Computational Fluid Dynamics Review 1996*, M.M. Hafez and K. Oshima, eds., John Wiley and Sons, West Sussex, UK.

[11] S.C. Chang, A. Himansu, C.Y. Loh, X.Y. Wang, S.T. Yu and P.C.E. Jorgenson, "Robust and Simple Non-Reflecting Boundary Conditions for the Space-Time Conservation Element and Solution Element Method", AIAA Paper 97-2077, to be presented at the 13th AIAA CFD Conference, June 29-July 2, 1997, Snowmass, CO.

[12] C.Y. Loh, S.C. Chang, J.R. Scott and S.T. Yu, "Application of the Method of Space-Time Conservation Element and Solution Element to Aeroacoustics Problems", Proceedings of the 6th International Symposium of CFD, September 1995, Lake Tahoe, NV.

[13] C.Y. Loh, S.C. Chang, J.R. Scott and S.T. Yu, "The Space-Time Conservation Element Method – A New Numerical Scheme for Computational Aeroacoustics", AIAA Paper 96-0276, presented at the 34th AIAA Aerospace Sciences Meeting, January 15-18, 1996, Reno, NV.

[14] C.Y. Loh, S.C. Chang and J.R. Scott, "Computational Aeroacoustics via the Space-Time Conservation Element / Solution Element Method", AIAA Paper 96-1687, presented at the 2nd AIAA/CEAS Aeroacoustics Conference, May 6-8, 1996, State College, PA.

[15] S.T. Yu and S.C. Chang, "Treatments of Stiff Source Terms in Hyperbolic Conservation Systems by the Method of Space-Time Conservation Element and Solution Element", AIAA Paper 97-0435, presented at the 35th AIAA Aerospace Sciences Meeting, January 1997, Reno, NV.

[16] S.T. Yu and S.C. Chang, "Application of the Space-Time Conservation Element and Solution Element Method to Chemically Reacting Flows", AIAA Paper 97-2099, to be presented at the 13th AIAA CFD Conference, June 29-July 2, 1997, Snowmass, CO.

[17] X.Y. Wang, C.Y. Chow and S.C. Chang, "Application of the Space-Time Conservation Element and Solution Element Method to Shock-Tube Problem", NASA TM 106806, December 1994.

[18] X.Y. Wang, "Computational Fluid Dynamics Based on the Method of Space-Time Conservation Element and Solution Element", Ph.D. Dissertation, 1995, Department of Aerospace Engineering, University of Colorado, Boulder, CO.

[19] X.Y. Wang, C.Y. Chow and S.C. Chang, "Application of the Space-Time Conservation Element and Solution Element Method to Two-Dimensional Advection-Diffusion Problems", NASA TM 106946, June 1995.

[20] X.Y. Wang, C.Y. Chow and S.C. Chang, "High Resolution Euler Solvers Based on the Space-Time Conservation Element and Solution Element Method", AIAA Paper 96-0764, presented at the 34th AIAA Aerospace Sciences Meeting, January 15-18, 1996, Reno, NV.

[21] X.Y. Wang, C.Y. Chow and S.C. Chang, "Numerical Simulation of Flows Caused by Shock-Body Interaction", AIAA Paper 96-2004, presented at the 27th AIAA Fluid Dynamics Conference, June 17-20, 1996, New Orleans, LA.

[22] X.Y. Wang, C.Y. Chow and S.C. Chang, "An Euler Solver Based on the Method of Space-Time Conservation Element and Solution Element", to appear in the Proceedings of the 15th International Conference on Numerical Methods in Fluid Dynamics, June 24-28, 1996, Monterey, CA.

[23] J.R. Scott and S.C. Chang, "A New Flux Conserving Newton's Method Scheme for the Two-Dimensional, Steady Navier-Stokes Equations", NASA TM 106160, June 1993.

[24] J.R. Scott, "A New Flux-Conserving Numerical Scheme for the Steady, Incompressible Navier-Stokes Equations", NASA TM 106520, April 1994.

[25] J. R. Scott and S.C. Chang, *Comp. Fluid Dyn.*, Vol. 5 (1995), pp. 189-212.

[26] J.R. Scott and S.C. Chang, "The Space-Time Solution Element Method – A New Numerical Approach for the Navier-Stokes Equations", AIAA Paper 95-0763, presented at the 33rd AIAA Aerospace Sciences Meeting, January 9-12, 1995, Reno, NV.

[27] J. R. Scott, "Further Development of a New, Flux-Conserving Newton Scheme for the Navier-Stokes Equations", NASA TM 107190, March 1996.

[28] D.A. Anderson, J.C. Tannehill and R.H. Pletcher, *Computational Fluid Mechanics and Heat Transfer*, 1984. Hemisphere Publ. Corp., New York.

[29] G.D. Smith, *Numerical Solution of Partial Differential Equations: Finite Difference Methods*, 3rd ed., 1985. Oxford Univ. Press, New York.

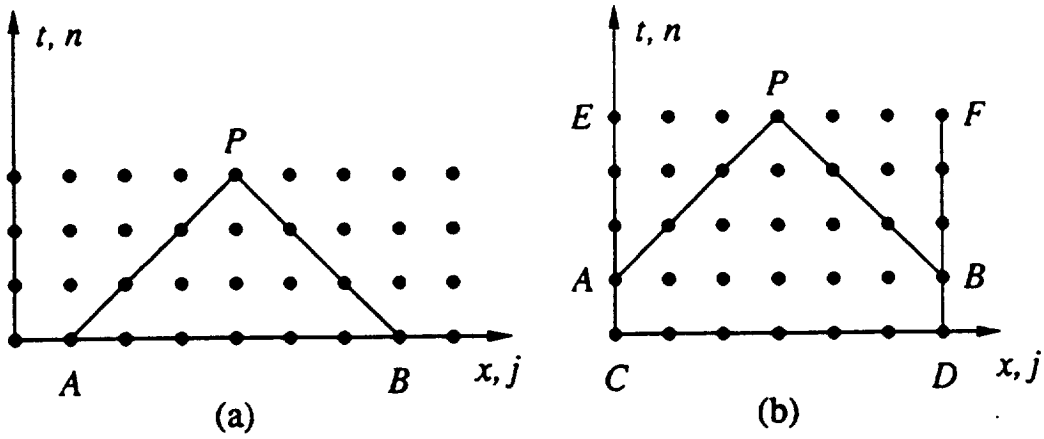

Figure 1 — (a) an initial-value problem
(b) an initial-value/boundary-value problem

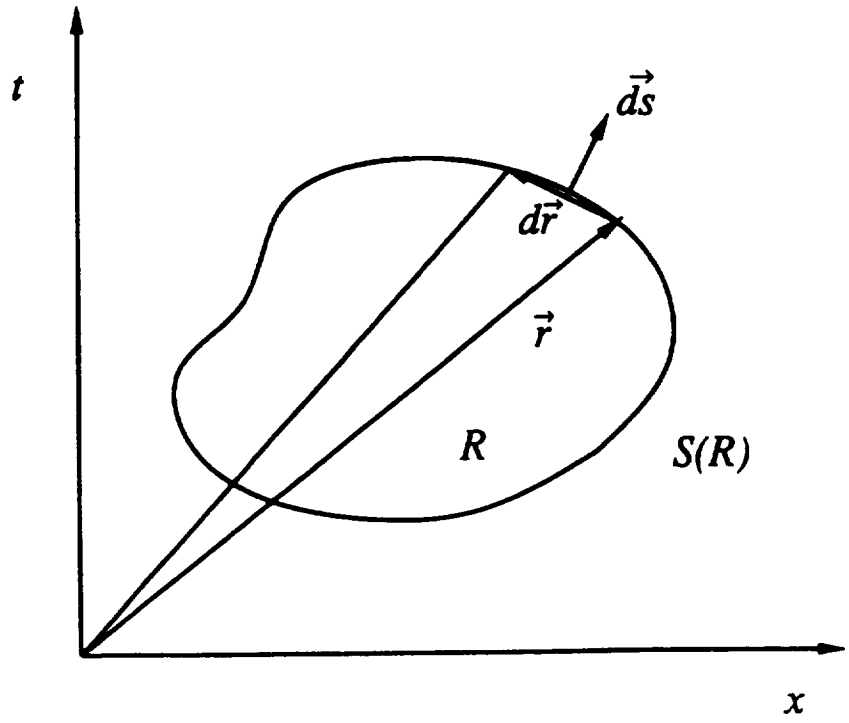

Figure 2 — A space-time conservation element with an arbitrary space-time domain

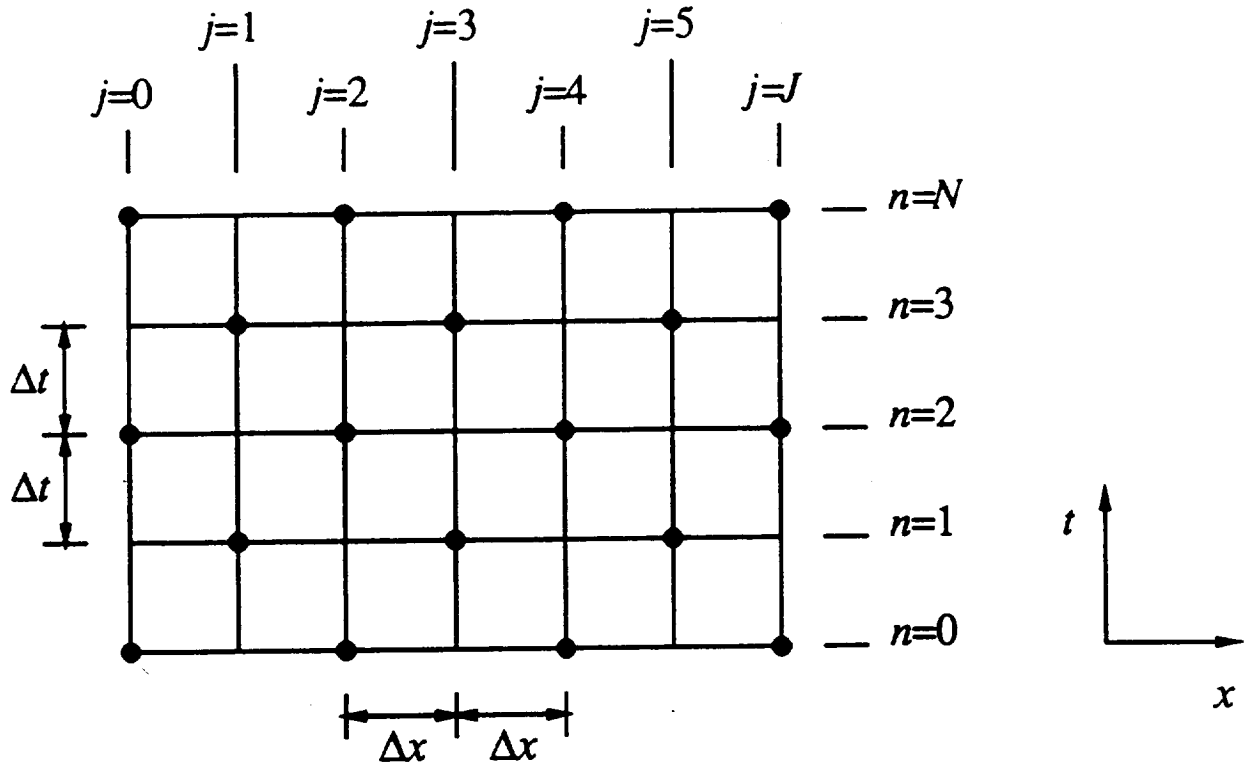

Figure 3 — The space-time mesh of the *a* scheme

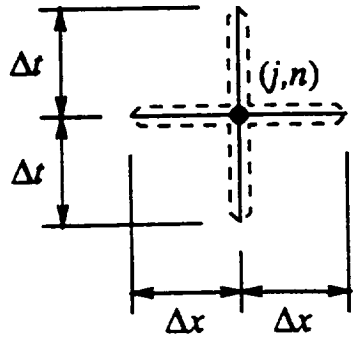

Figure 4 — SE(j,n)

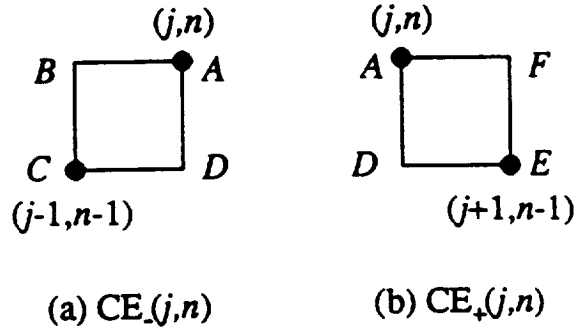

Figure 5 — The CEs associated with the mesh point (j,n)

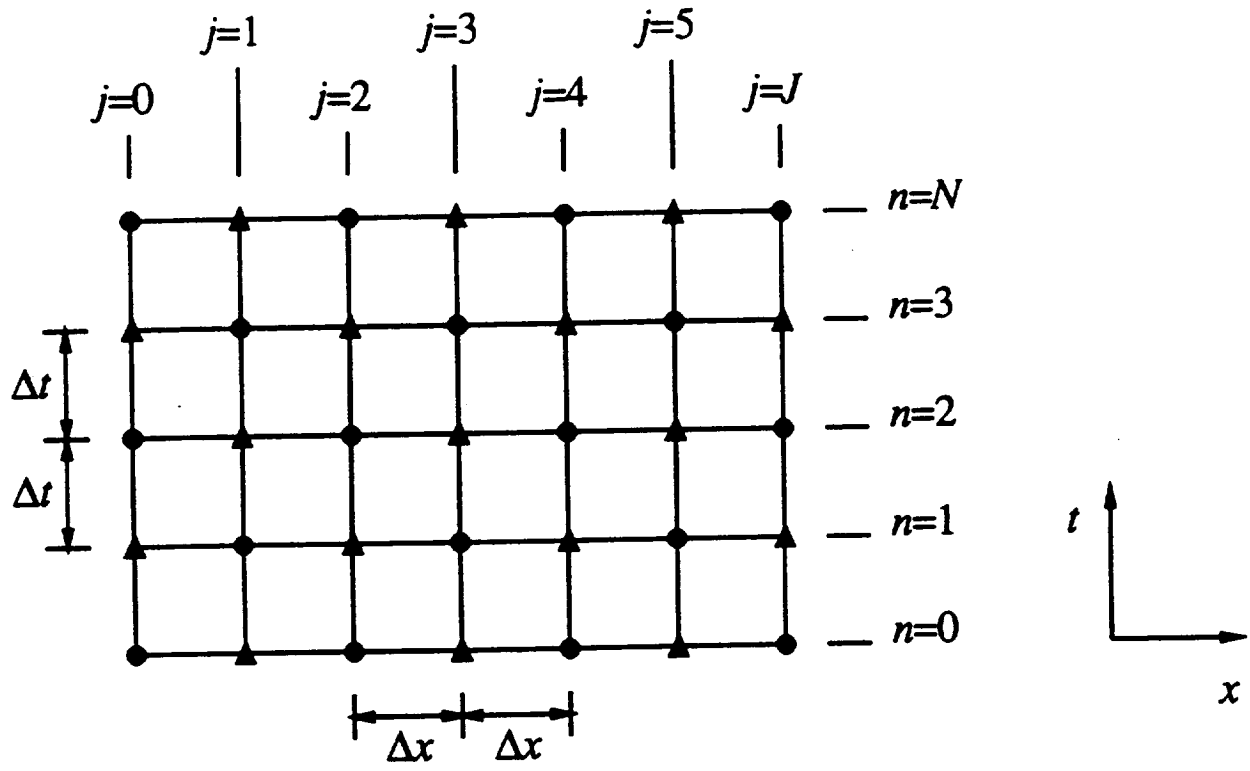

Figure 6 — The space-time mesh of the implicit schemes

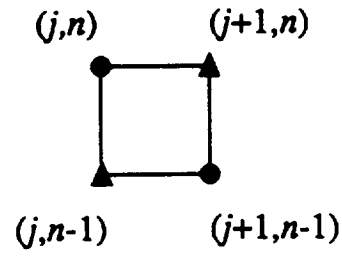

Figure 7 — A rectangular space-time region
shared by $CE_{-}(j+1,n)$ and $CE_{+}(j,n)$

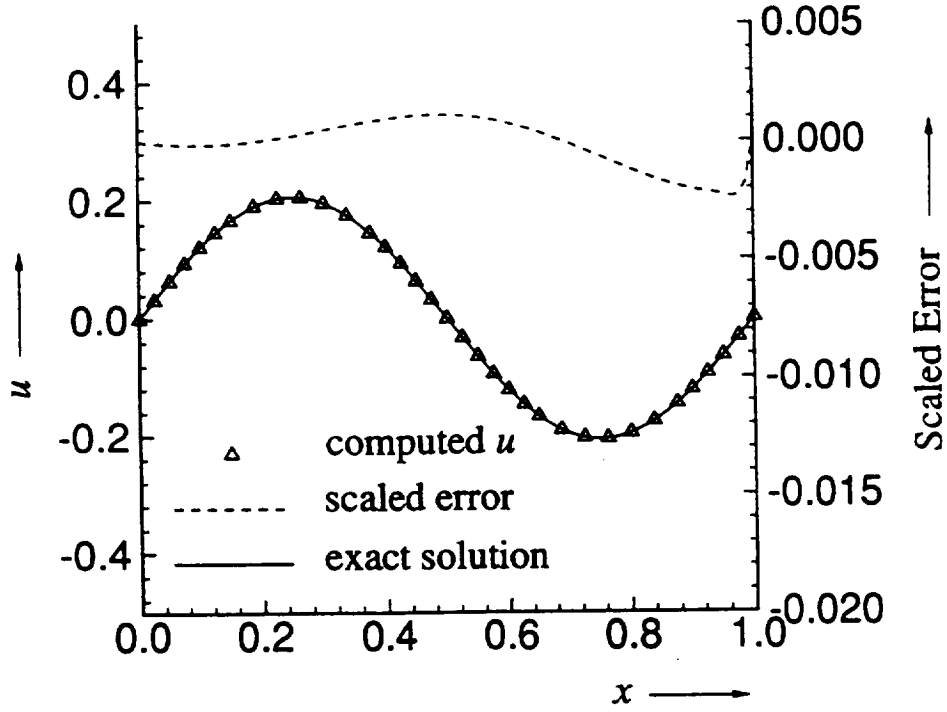

Figure 8 — a-μ ($I1$) Scheme : Sine Wave Example

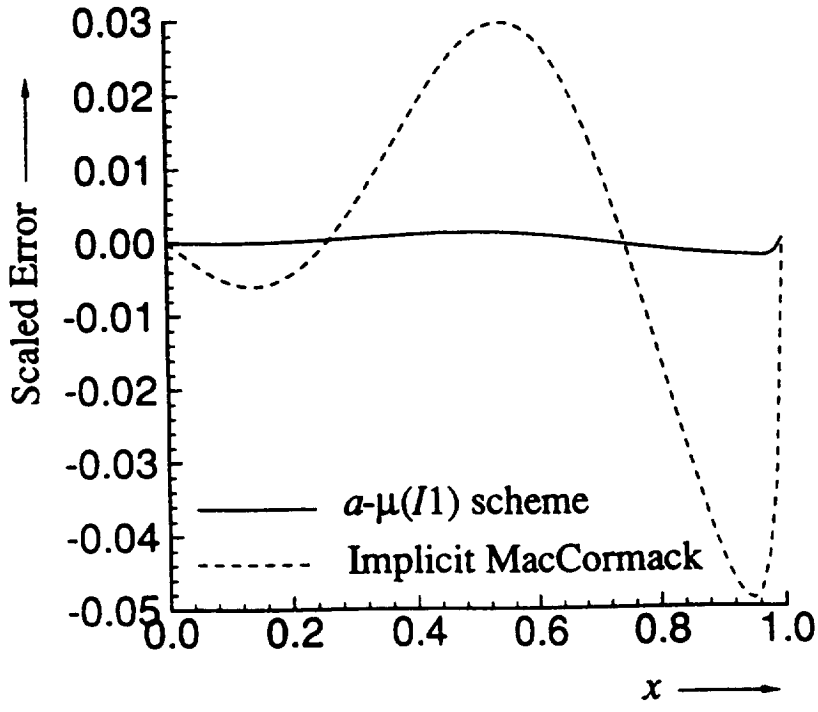

Figure 9 — Sine Wave Example : Comparison of Schemes

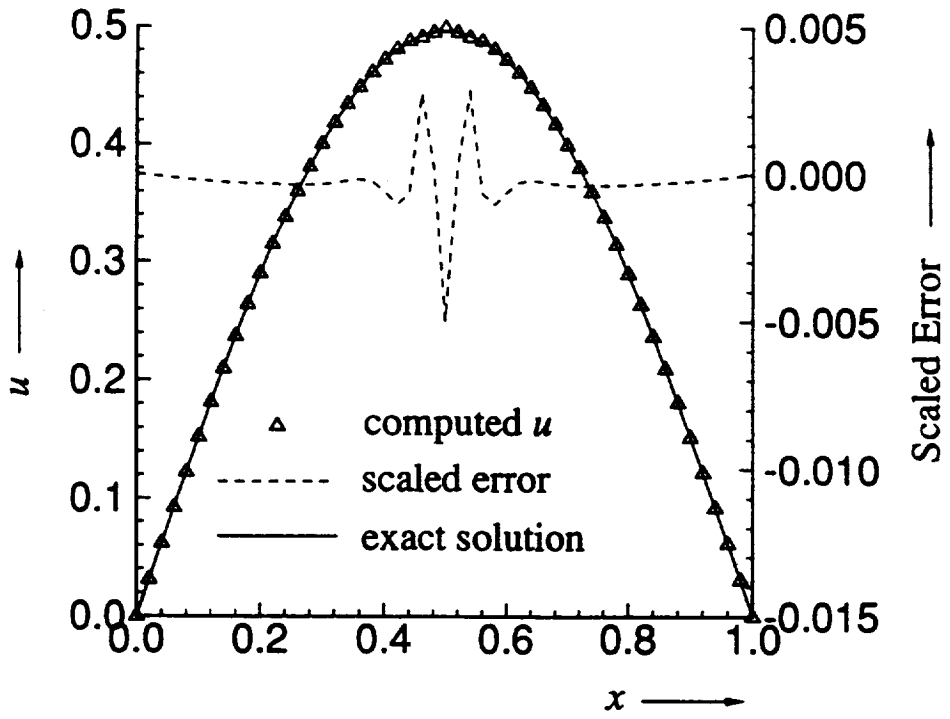

Figure 10 — a-μ ($I1$) Scheme : Pure Diffusion Example

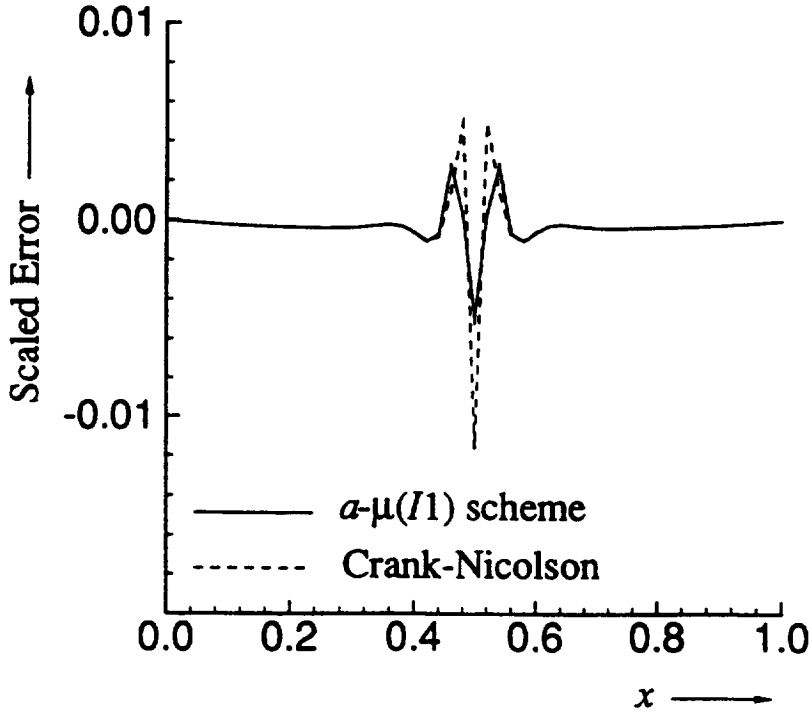

Figure 11 — Pure Diffusion : Comparison of Schemes

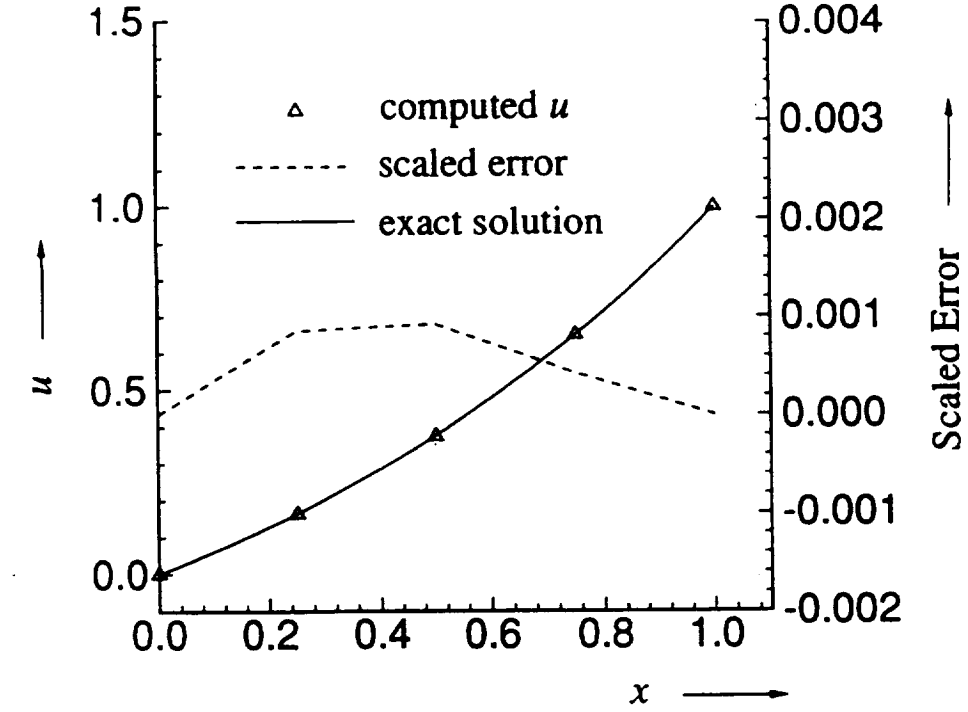

Figure 12 — a-μ ($I1$) Scheme : Boundary Layer, $Re = 1$

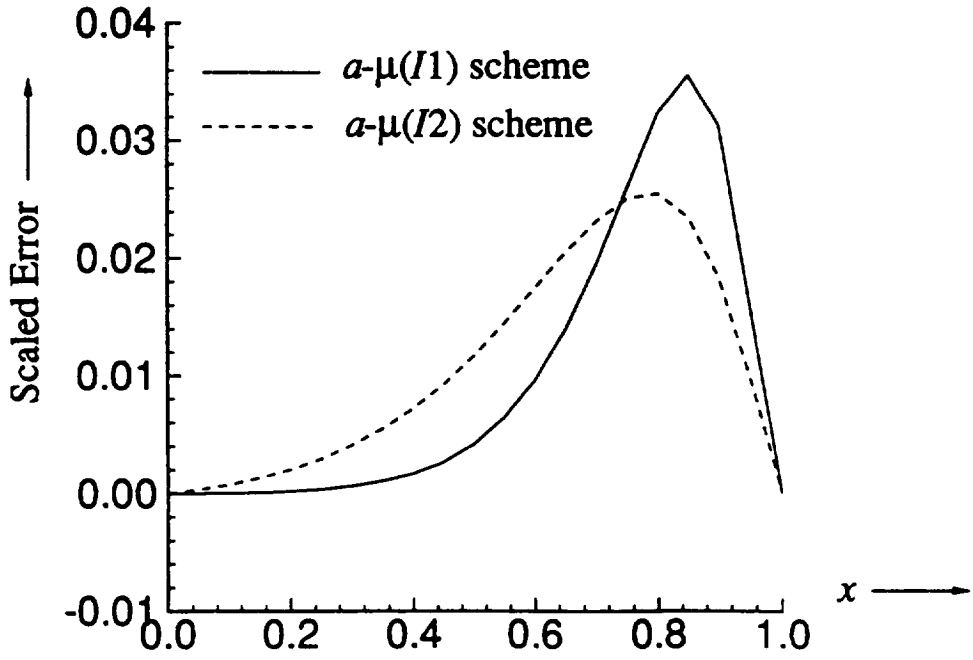

Figure 13 — Boundary Layer, $Re = 10$:
Comparison of Schemes

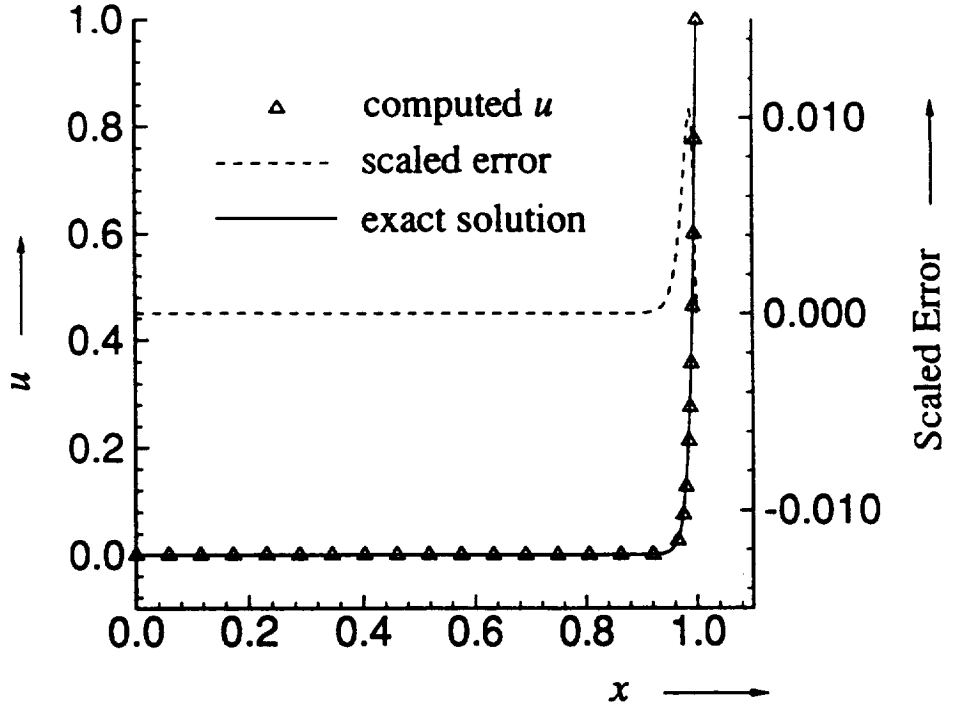

Figure 14 — a-μ ($I1$) Scheme : Boundary Layer, $Re = 100$

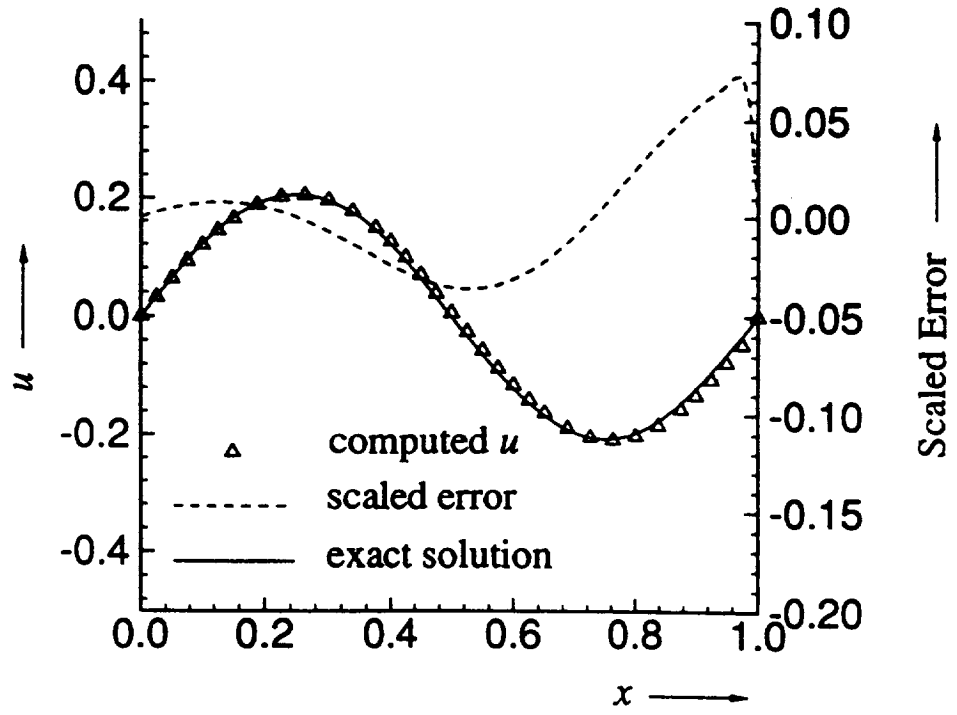

Figure 15 — Dual-Mesh Explicit a-μ Scheme Result

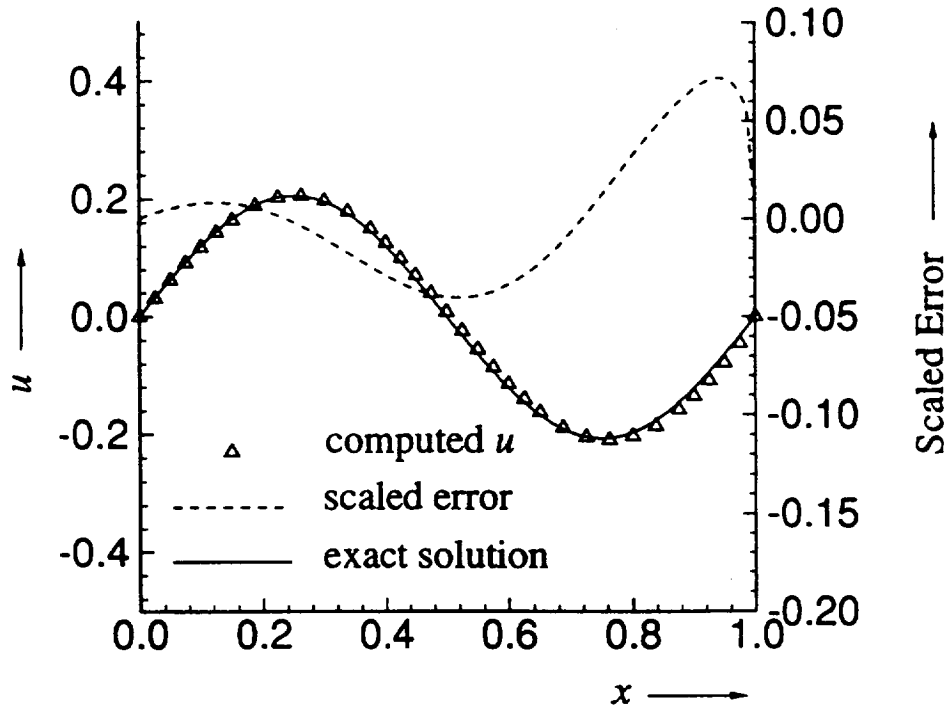

Figure 16 — Explicit *a*-μ Scheme (Ref. [6]) Result

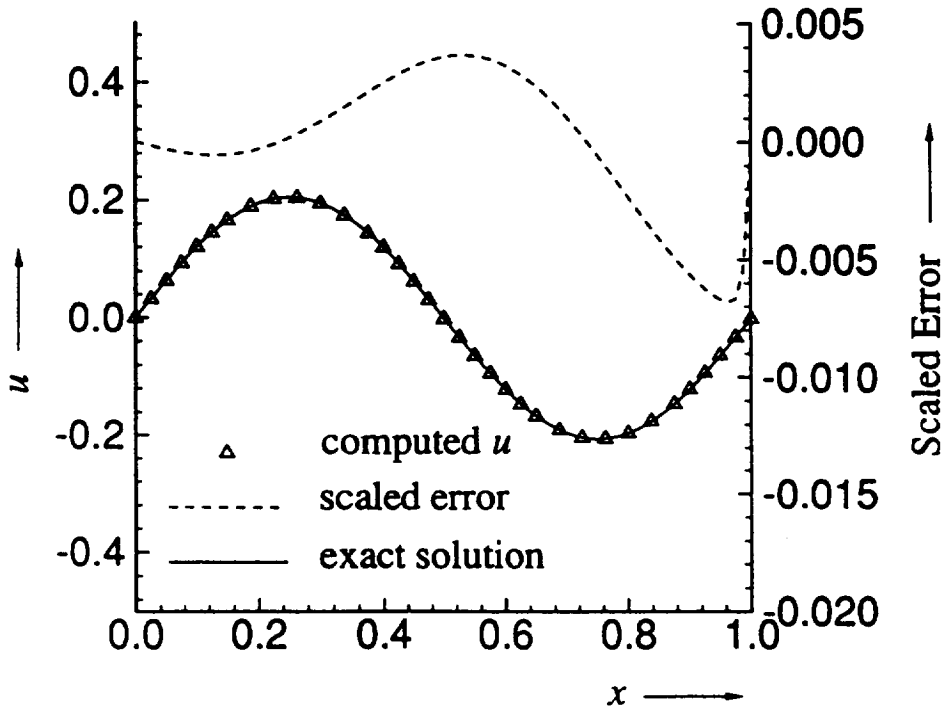

Figure 17 — Dual-Mesh Explicit *a*-μ Scheme, ν=0.2

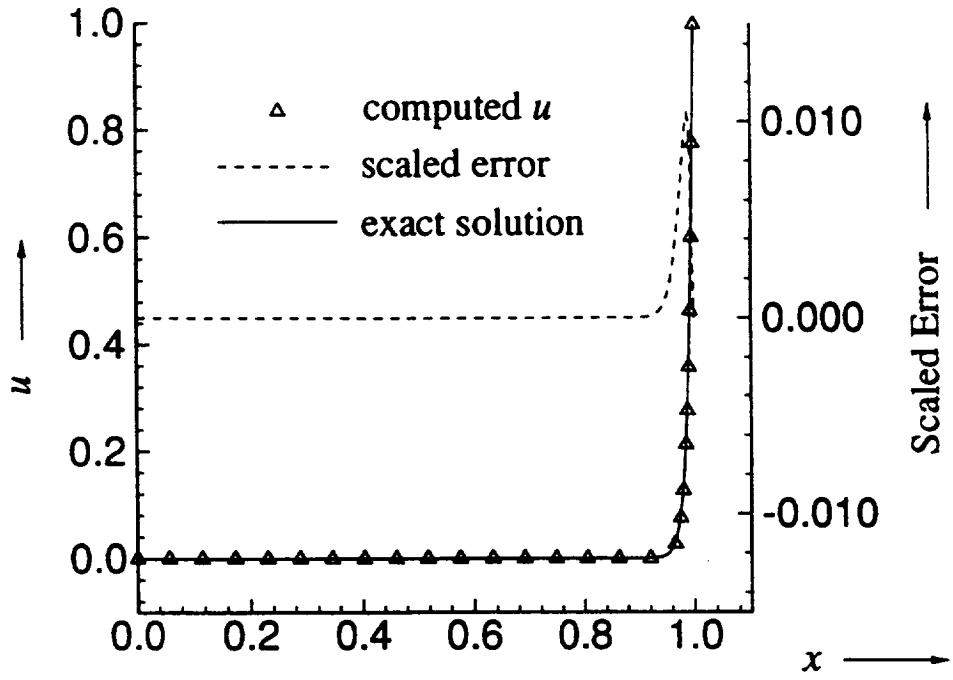

Figure 18 — Dual-Mesh Explicit a-μ Scheme : Boundary Layer, $Re = 100$

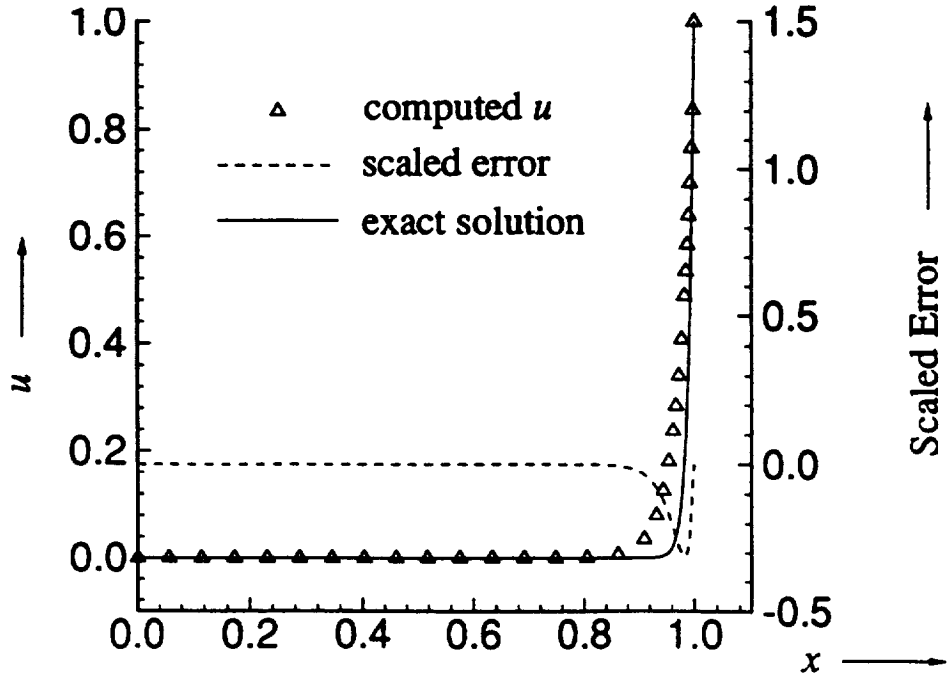

Figure 19 — Explicit a-μ Scheme (Ref. [6]) : Boundary Layer, $Re = 100$

REPORT DOCUMENTATION PAGE

Form Approved
OMB No. 0704-0188

1. AGENCY USE ONLY (*Leave blank*)	2. REPORT DATE	3. REPORT TYPE AND DATES COVERED
	November 1997	Technical Memorandum

4. TITLE AND SUBTITLE

The Implicit and Explicit α–μ Schemes

5. FUNDING NUMBERS

WU–523–26–23–00

6. AUTHOR(S)

Sin-Chung Chang and Ananda Himansu

7. PERFORMING ORGANIZATION NAME(S) AND ADDRESS(ES)

National Aeronautics and Space Administration
Lewis Research Center
Cleveland, Ohio 44135–3191

8. PERFORMING ORGANIZATION REPORT NUMBER

E–11005

9. SPONSORING/MONITORING AGENCY NAME(S) AND ADDRESS(ES)

National Aeronautics and Space Administration
Washington, DC 20546–0001

10. SPONSORING/MONITORING AGENCY REPORT NUMBER

NASA TM—97-206307

11. SUPPLEMENTARY NOTES

Sin-Chung Chang, NASA Lewis Research Center and Ananda Himansu, Cleveland Telecommunications Corporation, Solon, Ohio 44139. Responsible person, Sin-Chung Chang, organization code 5880, (216) 433–5874.

12a. DISTRIBUTION/AVAILABILITY STATEMENT

Unclassified - Unlimited
Subject Categories: 64 and 34 Distribution: Nonstandard

This publication is available from the NASA Center for AeroSpace Information, (301) 621–0390.

12b. DISTRIBUTION CODE

13. ABSTRACT ***(Maximum 200 words)***

Artificial numerical dissipation is an important issue in large Reynolds number computations. In such computations, the artificial dissipation inherent in traditional numerical schemes can overwhelm the physical dissipation and yield inaccurate results on meshes of practical size. In the present work, the space-time conservation element and solution element method is used to construct new and accurate numerical schemes such that artificial numerical dissipation will not overwhelm physical dissipation. Specifically, these schemes have the property that numerical dissipation vanishes when the physical viscosity goes to zero. These new schemes therefore accurately model the physical dissipation even when it is extremely small. The method of space-time conservation element and solution element, currently under development, is a nontraditional numerical method for solving conservation laws. The method is developed on the basis of local and global flux conservation in a space-time domain, in which space and time are treated in a unified manner. Explicit solvers for model and fluid dynamic conservation laws have previously been investigated. In this paper, we introduce a new concept in the design of implicit schemes, and use it to construct two highly accurate solvers for a convection-diffusion equation. The two schemes become identical in the pure convection case, and in the pure diffusion case. The implicit schemes are applicable over the whole Reynolds number range, from purely diffusive equations to purely inviscid (convective) equations. The stability and consistency of the schemes are analyzed, and some numerical results are presented. *It is shown that, in the inviscid case, the new schemes become explicit and their amplification factors are identical to those of the Leapfrog scheme. On the other hand, in the pure diffusion case, their principal amplification factor becomes the amplification factor of the Crank-Nicolson scheme.* We also construct an explicit solver with the treatment of diffusion being based on that in the implicit solvers. The explicit solver has only a CFL stability limitation on the Courant number, yet it retains the second-order spatial accuracy of the implicit schemes.

14. SUBJECT TERMS	15. NUMBER OF PAGES
Space-time; Conservation element; Solution element	60
	16. PRICE CODE: A04

17. SECURITY CLASSIFICATION OF REPORT	18. SECURITY CLASSIFICATION OF THIS PAGE	19. SECURITY CLASSIFICATION OF ABSTRACT	20. LIMITATION OF ABSTRACT
Unclassified	Unclassified	Unclassified	